

Pensieve: Retrospect-then-Compare Mitigates Visual Hallucination

Dingchen Yang¹, Bowen Cao², Guang Chen¹, and Changjun Jiang¹

¹ Tongji University

{dingchen_yang, guangchen, cjjiang}@tongji.edu.cn

² Peking University

cbw2021@stu.pku.edu.cn

Abstract. Multi-modal Large Language Models (MLLMs) demonstrate remarkable success across various vision-language tasks. However, they suffer from visual hallucination, where the generated responses diverge from the provided image. Are MLLMs oblivious to the accurate visual cues when they hallucinate? Our investigation reveals that the visual branch may equally advocate both accurate and erroneous content. To address this issue, we propose *Pensieve*³, a training-free method that leverages the analogous visual hallucinations, which are induced by images sharing common semantic and appearance characteristics, to mitigate hallucination. Specifically, *Pensieve* enables MLLMs to retrospect relevant images as references and compare their visual content with the test image via confidence score subtraction. Moreover, our paradigm balances the effects of addressing errors from both the visual and textual branches by adaptively scaling the subtracted scores. Experiments on Whoops, LLaVA Bench, POPE, and MME demonstrate the efficacy of *Pensieve* in mitigating visual hallucination, surpassing other advanced decoding strategies. *Pensieve* also aids MLLMs in identifying visual details and enhance the specificity of generated image descriptions.

Keywords: Visual Hallucination · Multi-modal Large Language Model

1 Introduction

Multi-modal Large Language Models (MLLMs) have emerged as dominant forces in vision-language tasks [6, 11, 29, 35, 38, 47, 62, 64, 69, 70, 76], showcasing remarkable advancements in comprehending a wide array of visual concepts.

Despite their impressive capabilities, state-of-the-art MLLMs are susceptible to visual hallucination [4, 9, 19–21, 27, 36, 37, 46, 48, 53, 60, 61, 75], wherein they inaccurately describe the visual inputs. Specifically, MLLMs can generate conflicting or fabricated content that diverges from the provided image, and may overlook crucial visual details. Examples illustrating this issue are presented in Fig. 1. Throughout this paper, we refer to the generated tokens (word or subword) containing inaccurate semantics as hallucinatory tokens.

³ Code is available at <https://github.com/DingchenYang99/Pensieve>.

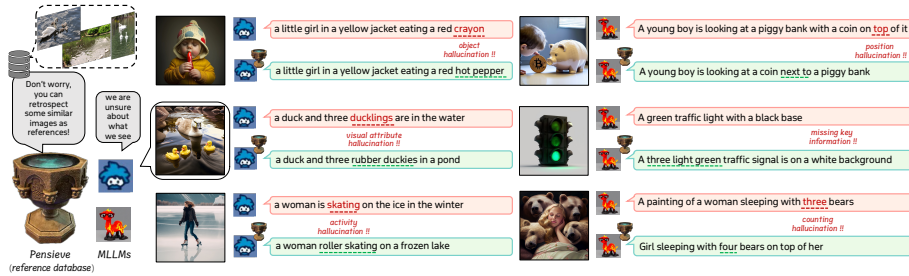


Fig. 1: Visual hallucinations in image captions and an illustration of our proposed method *Pensieve*. During inference, MLLMs are enabled to retrospect relevant images as references and compare their visual content with the test image. *Pensieve* is capable of correcting erroneous object categories, attributes, activities, position, and numbers, wherever they occur in the sentence. *Pensieve* also facilitates MLLMs to identify visual details in the image (e.g., the traffic light with three green lights).

Understanding the genesis of visual hallucinations is paramount for hallucination reduction. Previous studies underline flaws within MLLMs, such as under-distinctive visual features [48], the image-text modality gap [20, 46], biased feature aggregation patterns [19, 26, 53], and fitting superficial language priors in the training data [27, 75]. While these flaws impede MLLMs from accurately comprehending images, our investigation suggests a different perspective, that MLLMs may *not* be completely unaware of the accurate visual cues when they hallucinate; instead, their predictions reveal an uncertainty between accurate and hallucinatory content. Specifically, we observe that MLLM’s visual branch tends to equally advocate both the accurate and erroneous token candidates, which we term *visually deceptive candidates*, by contributing close confidence scores to them. This ambiguity can lead to visual hallucination.

The most straightforward approach to discern the accurate candidates from the visually deceptive ones is directly adjusting the predicted confidence score distribution, prioritizing the faithful content over hallucinations. However, this objective is beyond the scope of existing distribution post-processors, predominantly the Contrastive Decoding based methods [15, 27, 71], which are adept at reducing the uni-modal bias embedded in the language decoder yet omit errors from the visual branch. Commence with a premise that similar images may induce analogous visual hallucinations, we step forward to analyze the confidence score distribution shift when replacing the test image with retrieved alternatives. We observe moderate changes in visually deceptive candidates’ scores, whereas the scores for accurate candidates exhibit more significant variations. Leveraging this phenomenon, we introduce a training-free approach *Pensieve*. During inference, MLLMs are enabled to retrospect pertinent images as references and compare them with the test image. Specifically, the confidence scores predicted by the test image and retrieved references are subtracted to promote the candidates with sharp score variations, which are *less* likely to be the *visually deceptive candidates*. Moreover, *Pensieve* retains the capability in debiasing

erroneous language priors, and balances its effect in addressing errors from the visual and textual branches by adaptively scaling the subtracted scores.

We validate *Pensieve*'s effectiveness in mitigating visual hallucination on image captioning and Visual Question Answering (VQA) tasks. Quantitative and qualitative results on four benchmarks, Whoops [3], LLaVA Bench in the wild [39], MME [16], and POPE [32] demonstrate the superiority of *Pensieve*, notably increasing the FaithScore [21] by 0.4 for LLaVA1.5 [38] on Whoops, and the total score by 55 for InstructBLIP [11] on MME. Additionally, *Pensieve* helps MLLMs identify visual details and generate more specified image descriptions.

Our main contributions are three-fold:

- We empirically reveal that MLLMs are sometimes *aware* of accurate visual cues amidst visual hallucination, and analogous visual hallucinations can occur among similar images, which can be leveraged to mitigate hallucination.
- we introduce *Pensieve*, a novel paradigm that allows MLLMs to retrospect similar images as references, and discern accurate visual cues through comparing confidence scores predicted by the visual references. Moreover, the subtracted scores are adaptively scaled to balance the effect in mitigating hallucinations stemming from MLLMs' visual or textual branch.
- Experiments on image captioning and VQA demonstrate the superiority of *Pensieve*, *e.g.*, +0.4 FaithScore on Whoops for LLaVA1.5, and +55 total scores on MME for InstructBLIP. Qualitative results demonstrate that *Pensieve* also enhances the specificity of image descriptions.

2 Related works

2.1 Visual Hallucination and their Origins

Visual hallucination [37] refers to the issue wherein the descriptive content diverges from the visual input. These erroneous responses may exhibit fabrication, contradictions, or scarce specificity to the provided image. Initial investigations primarily address object-level visual hallucination [32, 44, 75], focusing solely on inappropriate nouns. This problem is subsequently extended to a finer granularity [9, 16, 40, 48, 52, 58, 67], including errors in visual attributes, spatial relationships, physical states, activities, and numbers.

The origins of visual hallucination stem from various sources. Some highlight flaws in the visual encoder, such as limited image resolution [66], under-distinctive visual representations that lack visual details [48] or spatial information [9], and poor cross-modal representation alignment [20]. Others emphasize deficiencies within the language decoder, such as biased attention score distribution [19, 26, 53, 57], adherence to superficial syntactical patterns (*e.g.*, frequent answers [36], contextual co-occurrence of objects [27, 75], and activities [56]), the overwhelming parametric knowledge [45, 66], and error snowballing [65, 68, 75]. In this study, we investigate the genesis of visual hallucination, and find that

MLLM’s visual branch tends to equally advocate both the accurate and erroneous candidates. This observation suggests new perspectives that visual hallucination can be reduced *without* directly tackling MLLMs’ inherent deficiencies, saving enormous amount of labeling or training costs.

2.2 Mitigating Visual Hallucination

Parameter Tuning. methods include curating diverse multi-modal instruction tuning dataset [36], designing feedback systems [46,63], and the provision of extra supervisions [9,20]. Nonetheless, the training cost becomes prohibitive for large-scale MLLMs. Furthermore, excessive parameter tuning may impair strengths of MLLMs [9,36], when the training recipe is suboptimal.

Model Ensemble. Integrating knowledge from other models compensates for MLLMs’ shortcomings. Feasible methods include improving the object recognition accuracy through ensembling detectors [8,72], and obtaining distinctive features by ensembling multiple vision encoders [72]. Another line of work utilizes a language model to post-hoc revise visual hallucinations [61,75]. Key challenges within this paradigm include tailoring interfaces for various task-specific models, and automating their selection based on the hallucination categories.

Decoding Strategy. Adjusting the confidence score distribution straightforwardly is a more efficient approach compared to model training and ensemble. OPERA [19] directly discards the candidates that may skew subsequent content toward hallucination and reelect the others. VCD [27] and its variants [1,15,71] extends Contrastive Decoding (CD) [31,73], which aims to mitigate factual hallucinations in LLMs, to the vision domain. VCD distorts the visual input to amplify language priors, and downgrades the candidates advocated merely by the language priors through logits subtraction. Other CD based methods [5,55] also effectively reduce the erroneous language bias embedded in the decoder of MLLMs. However, hallucinations originating from the visual branch have remained unexplored. In this study, we investigate how the visual modality mistakenly promotes erroneous candidates, and propose a novel method *Pensieve* to mitigate hallucinations that stem from MLLMs’ visual or textual branch.

3 Delve into Visual Hallucination

In this section, we investigate the genesis of visual hallucination through an end-to-end approach. Commence with a fundamental question: to what extent are MLLMs unaware of accurate visual cues amidst hallucinations? We designed a token-by-token evaluation pipeline and present our findings.

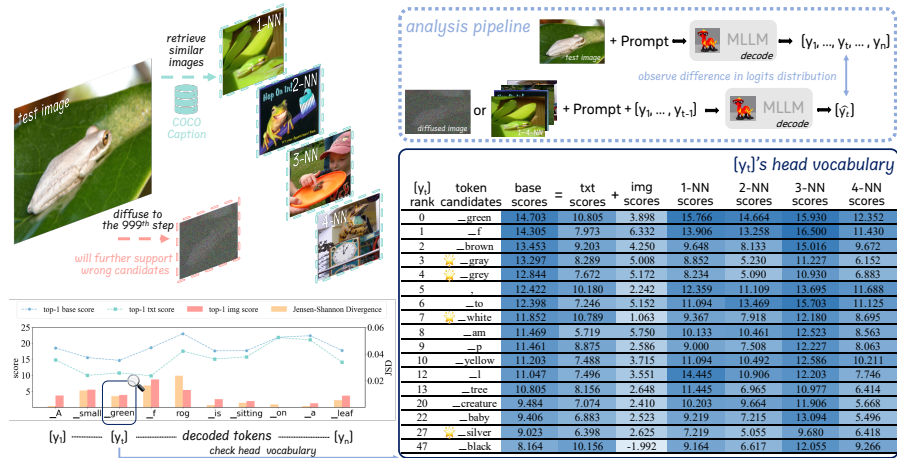


Fig. 2: Our visual hallucination analysis pipeline and results. We investigate LLaVA1.5’s predictions with alternative visual inputs in the same context. Such that the difference between y_t ’s and \hat{y}_t ’s confidence score distribution manifests the influence of the *visual* modality to MLLMs’ prediction. We find that LLaVA1.5 is aware of the accurate visual cues amidst hallucination, as the visual information contributed +5.008 scores for the accurate candidate *_gray*. However, the visual input also erroneously advocates for inaccurate candidates *_green* (+3.898) and *_brown* (+4.250). We also observe that images with similar semantics and appearance can induce analogous visual hallucinations, and leverage this phenomenon to assist MLLMs in discerning accurate content. This test sample is from OpenImages validation set [24].

Background. Leading MLLMs [6, 11, 35, 38, 62, 76] incorporate auto-regressive language models [49, 74], which repeatedly selects the next token from their vocabulary \mathcal{V} based on the probability of each token candidate x_i ,

$$p_\theta(x_i | \mathbf{v}, \mathbf{x}, \mathbf{y}_{<t}) = \frac{\exp(\mathbf{h}_t \cdot E_c(x_i))}{\sum_{x' \in \mathcal{V}} \exp(\mathbf{h}_t \cdot E_c(x'))} \quad (1)$$

where \mathbf{v} are the visual inputs, \mathbf{x} and $\mathbf{y}_{<t}$ are the prompt and past generated tokens, respectively. \mathbf{h}_t is the last hidden state predicted by the language model (also known as the next token feature). $E_c(x_i)$ is the token embedding of candidate x_i in the language head. (\cdot) is the inner product operator. The confidence score $\mathbf{h}_t \cdot E_c(x_i)$ embodies the degree of dominance of x_i ’s semantics in \mathbf{h}_t ⁴.

Analysis Pipeline. In this study, we pose the following questions: *When visual hallucination occurs, are MLLMs completely ignorant of the accurate visual cues? If not, can we help them distinguish the accurate content from hallucinations?* To address these inquiries, we aim to decouple the contribution of visual information

⁴ We find that for LLaVA1.5 and InstructBLIP, the mean L2 norm of all $E_c(x')$, for x' in \mathcal{V} , are close to 1. Thus the inner product result is close to the projection coordinate of the next token feature on a candidate’s embedding in the language model head.

in \mathbf{v} to the predicted confidence scores. Inspired by [33], we first input the test image \mathbf{v}^τ into the MLLM and greedily decode tokens $[y_1, \dots, y_n]$. At decoding step t , We denote y_t 's confidence score distribution as the *base scores*. Next, the test image is replaced with alternatives \mathbf{v}' (either a noised image without valid visual content, or other similar images), and the predicted tokens thus far $[y_1, \dots, y_{t-1}]$ are concatenated to \mathbf{x} to predict a new hidden state $\hat{\mathbf{h}}_t$ and decode \hat{y}_t , as illustrated in Fig. 2. We anticipate the input shift vectors $\Delta\mathbf{ve} = VE(\mathbf{v}^\tau) - VE(\mathbf{v}')$, *i.e.*, the change in input visual information, to induce a corresponding output feature shift $\Delta\mathbf{h} = \mathbf{h}_t - \hat{\mathbf{h}}_t$. Formally,

$$\mathbf{h}_t = LLM_\theta([VE(\mathbf{v}^\tau); TE(\mathbf{x}; \mathbf{y}_{<t})]) \quad (2)$$

$$\hat{\mathbf{h}}_t = LLM_\theta([VE(\mathbf{v}'); TE(\mathbf{x}; \mathbf{y}_{<t})]) \quad (3)$$

where VE denotes the visual encoder and adaptor. TE is the text embedding layer. Therefore, the confidence score distribution shift $\Delta\mathbf{h} \cdot E_c(x')$ for $x' \in \mathcal{V}$ (the subtraction of \hat{y}_t 's confidence scores from y_t 's) represents the semantics in \mathbf{h}_t contributed by the visual information in $\Delta\mathbf{ve}$.

3.1 MLLMs are not Blind amidst Hallucination

To integrally decouple the visual branch's contribution to the prediction, $\Delta\mathbf{ve}$ should encapsulate the *majority* of visual information present in the image. Following the diffusion process [18], we render the test image nearly indistinguishable from Gaussian noise. Then MLLM *blindly* predicts a new score distribution devoid of input visual cues (the *txt scores* in Fig. 2). Consequently, the subtraction of the blindly predicted *txt scores* from the original *base scores* can be interpreted as the contribution of the visual modality (the *img scores*).

Fig. 2 exhibits the multimodally distributed *img scores* across representative top-ranked candidates. Notably, both the accurate candidate (*e.g.*, *_gray*) and other erroneous candidates (*e.g.*, *_green*, *_brown* and *_yellow*) have relatively high *img scores*, indicating comparable advocacy from the visual branch. Therefore, the MLLM [38] is *not* completely ignorant⁵, but uncertain, to the accurate visual information when it hallucinates. We designate these inaccurate candidates, which are mistakenly advocated by the visual input, as *visually deceptive candidates*. Conversely, candidates with limited support, even opposition, from the visual branch are termed *textually deceptive candidates* (*e.g.*, candidate *_black* gets -1.992 *img scores*).

3.2 Visual References Help Discern Accurate Content

In the presence of both visually and textually deceptive candidates, implementing VCD [27], which adds scaled *img scores* to *base scores*, will further elevate the scores of the visually deceptive candidates *_green* and *_brown*, thereby

⁵ We quantify the extent of dependency of MLLMs' predictions on the visual input with the *img scores* and the Jensen-Shannon Divergence. Details are in Appendix.

exacerbating visual hallucination. In this case, it also risks depressing the specificity by further promoting candidate `_f` (first token of frog). We continue to explore feasible methods to help MLLMs discern these erroneous content. Start with an intuitive hypothesis that in the same context $\mathbf{x} + \mathbf{y}_{<t}$, images sharing similar semantics and appearance are likely to induce *analogous* visual hallucinations, we proceed by analyzing the scores predicted using retrieved images, which possess visual characteristics in common with the test image. We present four retrieved images from COCO-Caption [34], with corresponding predictions in the *k-NN scores* columns in Fig. 2.

Upon comparing the *base scores* with four *k-NN scores*, a notable observation emerges: the score of the accurate candidate `_gray` decreases significantly from 13.297 to 7.865 in average across four references. In contrast, the score change of visually deceptive (e.g., `_green`, `_brown`, and `_yellow`) and textually deceptive (e.g., `_black`) candidates are relatively modest (e.g., candidate `_green` scores 15.390 and 12.352 in images without green frogs, and candidate `_brown` also has relatively high scores in images without brown frogs). This observation suggests that in the same context, similar images can induce analogous visual hallucinations. Furthermore, token candidates whose scores vary significantly across similar images in the same context are *more likely to be the correct ones* than candidates with moderate changes. We leverage this phenomenon to discern accurate content and mitigate visual hallucination.

4 Methodology

Motivated by our observation that analogous hallucinations among similar images can help MLLMs discern accurate content, we propose a training-free and plug-and-play method *Pensieve*, which comprises two key components, searching similar images and contrasting visual cues.

4.1 Retrospect Visual Concepts

We aim to build a reference database that encompasses diverse visual concepts for MLLMs to retrospect. Concretely, our database contains samples from the COCO Caption [34] dataset, which covers a broad spectrum of daily and common visual content. Moreover, the visual references should be capable of *inducing* visual hallucinations, such that the analogous hallucinations can be further leveraged to reduce hallucination. Therefore, we include both the Karpathy [22] *train* and *restval* splits of COCO Caption. We posit that images from the *restval* split are more likely to induce visual hallucinations, as they are *not* included in the MLLMs’ training set [11, 38], and consequently benefit model performance. Specifically, we retrieves *k* most relevant visual references for each test sample *q* from the reference database \mathcal{D} , based on a similarity measure $\mathcal{F}(\cdot, \cdot)$. Formally,

$$\{r_1, \dots, r_k | q\} = \arg \max_k \{\mathcal{F}(E_R(s_j), E_R(q)) | s_j \in \mathcal{D}\} \quad (4)$$

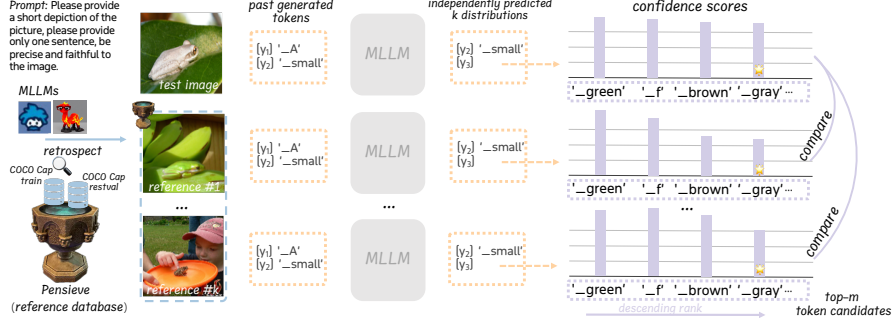


Fig. 3: Our approach identifies erroneous candidates that are mistakenly supported by the visual branch by leveraging the analogous visual hallucinations among similar images. Our reference database comprises a variety of images. During inference, relevant references are retrieved from this database, and MLLM generates distinct prediction for each reference in the same context. The predicted scores are then subtracted to highlight the accurate candidates.

where $E_R(\cdot)$ is the retriever that embeds the raw inputs into vector representations. $\mathcal{D}[r]$, $r \in \{r_1, \dots, r_k | q\}$, are the desired references for q . For image captioning, the visual feature $E_R(\mathbf{v})$ is used to retrieve images with similar semantics and appearance. In binary VQA task, we adapt our approach to find visual references that align with the semantic of the question using $E_R(\mathbf{x})$. We expect that comparing with such references will aid in reducing false positives (A detailed case study and discussion are in Appendix C.3).

4.2 Compare Visual Concepts

Contrasting with the confidence scores (denoted as *logits* in Eq. (5) and Eq. (8)) predicted by visual references can help distinguish accurate visual cues. As illustrated in Fig. 3, the MLLM generates $k + 2$ distinct predictions for each token candidate $x_i \in \mathcal{V}$, *i.e.*, from one test image \mathbf{v}^τ , one diffused image \mathbf{v}^d , and k retrieved images $\{\mathbf{v}^{NN}\}_k$, with identical textual prefix $\mathbf{x} + \mathbf{y}_{<t}$. Note that the context length is *not* increased in our paradigm, such that the computational burden is not significantly increased. We contrast x_i 's score corresponding to the test image \mathbf{v}^τ to the $k + 1$ references. Formally,

$$\begin{aligned}
 & \text{logits}(x_i | \mathbf{x}, \mathbf{y}_{<t}, \mathbf{v}^\tau, \mathbf{v}^d, \{\mathbf{v}^{NN}\}_k) \\
 &= (\alpha_\tau + \alpha_d^t + \alpha_{NN}^t) \text{logits}(x_i | \mathbf{x}, \mathbf{y}_{<t}, \mathbf{v}^\tau) \\
 & - \frac{\alpha_{NN}^t}{k} \sum_{j=1}^k \text{logits}(x_i | \mathbf{x}, \mathbf{y}_{<t}, \mathbf{v}_j^{NN}) - \alpha_d^t \text{logits}(x_i | \mathbf{x}, \mathbf{y}_{<t}, \mathbf{v}^d) \quad (5)
 \end{aligned}$$

The subtraction operator in Equation 5 underscores the difference between the test image and the visual references, thereby downgrading the analogous visual hallucinations across similar images. The retrieved images $\{\mathbf{v}^{NN}\}_k$ target at

reducing visually deceptive content, and \mathbf{v}^d aids in addressing textually deceptive hallucinations. The outcome of Eq. (5) is subsequently used for token selection, and this process is activated throughout the output sentence.

Adaptive Logits Processing. We regulate the influence of $\{\mathbf{v}^{NN}\}_k$ and \mathbf{v}^d to balance *Pensieve*’s effect in addressing errors from the visual and textual branches. Specifically, in cases where MLLMs exhibit uncertainty [75] regarding the recognized visual cues, *i.e.*, the scores $\{l_{i,t}^\delta\}_{i=0}^{m-1}$ calculated by Eq. (8) demonstrate multimodal distribution, then the coefficient α_d^t is reduced while α_{NN}^t is increased at the current decoding step t . This adjustment ensures that the visually deceptive candidates are not further endorsed. Formally,

$$\alpha_d^t = \beta_d \exp(\max(\text{softmax}(\{l_{i,t}^\delta\}_{i=0}^{m-1}))) \quad (6)$$

$$\alpha_{NN}^t = \beta_{NN} \exp(1 - \max(\text{softmax}(\{l_{i,t}^\delta\}_{i=0}^{m-1}))) \quad (7)$$

$$l_{i,t}^\delta = \text{logits}(x_i | \mathbf{x}, \mathbf{y}_{<t}, \mathbf{v}^\tau) - \text{logits}(x_i | \mathbf{x}, \mathbf{y}_{<t}, \mathbf{v}^d) \quad \text{s.t.} \quad x_i \in \mathcal{V}_{head}^m \quad (8)$$

Following the adaptive plausibility constraint [31], we only consider x_i that are among the top-ranked m candidates, *i.e.*, a fixed-length head vocabulary \mathcal{V}_{head}^m , which is selected based on the scores predicted from \mathbf{v}^τ . We set m to 50 for image captioning and 2 for binary VQA. α_τ , β_d and β_{NN} are hyper-parameters, which are by default set to 1.0, 0.1, and 0.1, respectively.

5 Experiments

General Settings. We evaluate *Pensieve* on image captioning benchmarks, including Whoops [3] and LLaVA-Bench [39], as well as on binary VQA benchmarks (MME [16] and POPE [32]), evaluating hallucinations in both generative and discriminative tasks. The effectiveness of each component is examined via ablation study. All experiments are in zero-shot manner, with LLaVA1.5-7B [38] and InstructBLIP-7B [11] as baseline models, both using Vicuna [74] as the language decoder⁶. We compare *Pensieve* with two advanced decoding strategies VCD [27] and DoLa [10]. We employ greedy decoding as the baseline strategy for reproducibility, and to avoid visual hallucinations induced by token sampling [25, 30, 53]. Implementation details and specific experimental settings for each benchmark are in the Appendix.

5.1 Image Captioning

In light of that MLLMs encode rich real-world conventions and may embed certain superficial syntactical patterns in model parameters [75], we assume that commonsense-violating images (see examples in Fig. 1) can highlight the problem of visual hallucination. For quantitative evaluation, we employ image captioning

⁶ <https://github.com/lm-sys/FastChat>

Table 1: Results on Whoops benchmark. *Pensieve* boosts the overall performance for LLaVA-1.5 and InstructBLIP. B4, M, C, S, and FS% refer to Bleu@4, METEOR, CIDEr, SPICE, and FaithScore, respectively. We copy the results of EVCap with and without retrieval augmentation.

Method	B4 ↑	M ↑	C ↑	S ↑	FS% ↑	
<i>further trained on COCO</i>						
EVCap [28] Vicuna-13B	24.1	26.1	85.3	17.7	-	
EVCap w/ RA [28] Vicuna-13B	24.4	26.1	86.3	17.8	-	
<i>zeroshot</i>						
LLaVA-1.5 [38] Vicuna-7B	greedy	19.7	25.6	67.9	17.3	67.9
	+DoLa	19.9	25.6	67.8	17.4	67.7
	+VCD	19.1	25.4	69.1	17.3	67.6
	+Ours	20.0	26.3	75.5	17.8	68.3
	greedy	24.9	26.5	87.3	18.2	74.1
InstructBLIP [11] Vicuna-7B	+DoLa	24.8	26.5	87.4	18.2	74.2
	+VCD	25.5	27.0	89.2	18.2	72.2
	+Ours	25.7	27.1	90.6	18.6	74.0

metrics BLEU [42], METEOR [12], CIDEr [51], and SPICE [2]. FaithScore [21] is utilized for automatic visual hallucination evaluation, which is calculated by ChatGPT and a visual entailment expert model OFA⁷ [54]. We also provide qualitative results on LLaVA Bench in the Wild [39] in Fig. 4 and in the Appendix to illustrate the efficacy of *Pensieve* in various image domains.

Quantitative Results on Whoops. Tab. 1 demonstrate that our proposed *Pensieve* contribute to a substantial improvement in all captioning metrics for both MLLMs, notably increasing the CIDEr score by 7.6 and the Faithscore by 0.4 for LLaVA1.5, surpassing DoLa and VCD in varying degrees. Furthermore, our retrospect-then-compare paradigm exhibits more pronounced improvements compared to the traditional retrieval-augmented (RA) image captioning paradigm EVCap [28], which relies on retrieved visual semantics to augment the input visual embeddings, and increases the CIDEr score by only 1.0.

Qualitative Results on LLaVA Bench. LLaVA Bench in the Wild evaluates the ability of MLLMs to comprehend diverse visual concepts, spanning indoor and outdoor scenes. Fig. 4 demonstrates that *Pensieve* effectively reduces visual hallucinations at varying granularity for both MLLMs, *e.g.*, it helps LLaVA1.5 correctly describe the spatial relationship between the milk, yogurt, and strawberries in the same refrigerator compartment; and help InstructBLIP identify the cars near the beach. In these complex scenarios, VCD and DoLa struggle to assist MLLMs in discerning non-existent content, and may induce additional errors, *e.g.*, the cars and the boats. More examples are in the Appendix.

⁷ <https://github.com/OFA-Sys/OFA>



Fig. 4: Qualitative results on LLaVA-Bench in the wild. *Pensieve* effectively mitigates visual hallucination for both MLLMs, while VCD and DoLa may induce extra hallucinations. We present the test images with corresponding visual references, which illustrate a similar scenario but exhibit nuanced differences compared to the test image. We omit DoLa’s result for LLaVA1.5 as it is identical to the original one.

5.2 Visual Question Answering

We further evaluate *Pensieve* on binary VQA benchmarks, which are designed to gauge the extent of visual hallucination in a yes-or-no discriminative manner. To prevent information leakage, we exclude all images that appeared in MME and POPE from the reference database, such that the test samples themselves do not serve as references.

Results on MME. Following previous works [27, 61], we present results on the hallucination subset of MME in Tab. 2, including Color, Count, Existence, and Position subtasks. We report the officially defined metric that combines accuracy and accuracy+. *Pensieve* improves the total score for both LLaVA1.5 (+10) and InstructBLIP (+55), surpassing DoLa and VCD in average by 33.4 and 33.3 scores, respectively. In particular, *Pensieve* effectively mitigates visual hallucination in color-related perception task for both MLLMs (+10 scores for LLaVA1.5 and noticeably +33.3 scores for InstructBLIP).

Results on POPE. We present the averaged Accuracy and F1 score across the random, popular, and adversarial splits in Tab. 3. On three subsets of POPE, *Pensieve* boosts the overall Accuracy of both LLaVA1.5 (+0.25 in avg.) and InstructBLIP (+0.91 in avg.), outperforming VCD by 1.85 for LLaVA1.5 and by 1.12 for InstructBLIP, respectively. It is worth noticing that greedy decoding avoids errors stemming from token sampling, especially when the MLLMs’ predictions have high perplexity, thus significantly surpassing the multi-nominal sampling strategy reported in VCD.

5.3 Ablation Studies

We validate the effectiveness of each component in *Pensieve* by individually ablating them, and evaluating the performance variation on image captioning task

Table 2: Results on the hallucination subset of the MME benchmark (Color, Count, Existence, and Position subtasks). *Pensieve* elevates the total score for both MLLMs. Results of all perception subtasks are in the Appendix.

Model	Decoding	Color ↑	Count ↑	Exist. ↑	Pos. ↑	Total ↑
LLaVA-1.5	greedy	155.0	158.3	195.0	123.3	631.7
	+ <i>DoLa</i>	153.3	158.3	195.0	123.3	630.0
	+ <i>VCD</i>	148.3	158.3	190.0	126.7	623.3
	+ <i>Ours</i>	165.0	153.3	195.0	128.3	641.7
InstructBLIP	greedy	120.0	60.0	185.0	50.0	415.0
	+ <i>DoLa</i>	120.0	60.0	185.0	50.0	415.0
	+ <i>VCD</i>	123.3	60.0	185.0	53.3	421.7
	+ <i>Ours</i>	153.3	78.3	180.0	58.3	470.0

Table 3: Results on the POPE benchmark. *Pensieve* demonstrates superior performance to VCD and DoLa on MSCOCO, AOKVQA and GQA subsets.

Model	Decoding	COCO		AOKVQA		GQA	
		Acc. ↑	F1 ↑	Acc. ↑	F1 ↑	Acc. ↑	F1 ↑
LLaVA-1.5	greedy	85.56	84.11	84.32	84.40	84.73	84.84
	+ <i>DoLa</i>	85.38	83.86	84.30	84.33	84.71	84.76
	+ <i>VCD</i>	85.59	85.53	82.07	83.39	82.17	82.87
	+ <i>Ours</i>	85.80	84.58	84.56	84.91	85.01	85.38
InstructBLIP	greedy	85.14	84.45	81.73	83.18	80.58	82.03
	+ <i>DoLa</i>	85.21	84.54	81.74	83.22	80.56	82.03
	+ <i>VCD</i>	84.42	83.62	81.50	82.78	80.90	82.05
	+ <i>Ours</i>	85.12	84.37	83.30	83.88	81.76	82.15

(the Whoops benchmark). The impact of the reference database is investigated by adding or removing the data samples. We also conduct a case study on how *Pensieve* improves performance on binary VQA task in Appendix C.3.

Similar Images are Better than Random. We first ablate the image retrieval process (abbreviated img. ret.), randomly sampling four images from the reference database instead. The averaged results and the standard deviations of five separate runs are shown in Exp.3. The results suggest that random images can have positive effects (+4.5 CIDEr score and +0.3 SPICE score compared to Exp.1), highlighting the robustness of *Pensieve* in scenarios where similar images are absent. We present the random and retrieved images in Fig. 5 to illustrate the difference in similarity between visual references. Moreover, when similar images are available (Exp.2), *Pensieve* contribute to a more significant performance gain across all metrics (CIDEr +7.6 and SPICE +0.5). Note that we retain the diffused image as it helps debias certain erroneous language priors, and the CIDEr score dropped by 2.3 in Exp.4 after the diffused image is ablated.

Visual Concepts Comparison is Better than Combination. We fix hyperparameters and alter the visual concept comparison process (abbreviated comp.), transitioning from logits subtraction to addition in Eq. (5), *i.e.*, emphasizing

Table 4: Ablation study on the Whoops benchmark. Each component in *Pensieve* has a positive impact on the overall performance. All experiments use LLaVA-v1.5-7B as the MLLM (Exp.1). Results of *Pensieve* are in Exp.2. The performance gap to Exp.2 are presented for Exp.3 to 9, which are marked in **green** or **red**.

Exp.	img. ret.	diffuse img.	comp.	adapt.	num. refs	B4 ↑	M ↑	C ↑	S ↑	FS% ↑
1					n/a	19.7	25.6	67.9	17.3	67.9
2	✓	✓	✓	✓	4	20.0	26.3	75.5	17.8	68.3
3	rand.	✓	✓	✓	4	18.7 ^{±0.3} _(-1.3)	26.0 ^{±0.1} _(-0.3)	72.4 ^{±0.7} _(-3.1)	17.6 ^{±0.1} _(-0.2)	67.1 ^{±0.3} _(-1.2)
4	✓		✓	✓	4	20.1 ^(+0.1)	26.2 ^(-0.1)	73.2 ^(-2.3)	17.9 ^(+0.1)	69.0 ^(+0.7)
5	✓	✓	add.	✓	4	17.6 ^(-2.4)	23.4 ^(-2.9)	58.7 ^(-16.8)	16.3 ^(-1.5)	66.9 ^(-1.4)
6	✓	✓	✓		4	19.9 ^(-0.1)	26.3 ^(-0.0)	71.9 ^(-3.6)	17.7 ^(-0.1)	68.9 ^(+0.6)
7	✓	✓	✓	✓	1	19.4 ^(-0.6)	26.3 ^(-0.0)	73.8 ^(-1.7)	17.5 ^(-0.3)	66.0 ^(-2.3)
8	✓	✓	✓	✓	2	19.8 ^(-0.2)	26.3 ^(-0.0)	74.6 ^(-0.9)	17.7 ^(-0.1)	67.5 ^(-0.8)
9	✓	✓	✓	✓	8	20.2 ^(+0.2)	26.4 ^(+0.1)	76.5 ^(+1.0)	17.9 ^(+0.1)	67.6 ^(-0.7)

the common visual cues among various images. Exp.5 demonstrates notable decreases in all metrics (*e.g.*, CIDEr -16.8), indicating that the additive paradigm can harm the language modeling process. This result validates that contrasting visual concepts is better than combining them.

The Size and Content of the Reference Database. We investigate the impact of the reference database’s size on model performance by incorporating more (110k) images from the Visual Genome [23] dataset. Upon doubling the size, we observe slight decrease in all metrics, *e.g.*, CIDEr score decreases from 75.5 to 74.6, and more dissimilar visual content within the retrieved images (*e.g.*, a frisbee in Fig. 5). Consequently, enlarging the database necessitates extra effort to filter out noisy retrieval results. We also validate our hypothesis that images excluded in the training process can enhance performance. We build two reference databases with images from the Karpathy *train* or *restval* split only. Notably, utilizing references merely from the *restval* split yields the highest image captioning performance (77.0 CIDEr score and 18.0 SPICE score, as shown in the *CocoV* column in Fig. 5), outperforming the counterpart with the *train* split only (CIDEr 75.8 and SPICE 17.8). However, combining samples from the *train* and *restval* splits yields the best FaithScore (68.3).

Other Ablations. Exp.6 demonstrate that the adaptive (abbreviated adapt.) logit processing scheme can enhance all metrics (except for the FaithScore). Besides, increasing the number of reference images provides steady improvement in image captioning performance (CIDEr score increases from 73.8 to 76.5 in Exp.7-9). We use four references by default.

6 Limitation

Pensieve operates on the premise that in the same context, images with similar semantics and appearance are likely to induce analogous visual hallucinations.

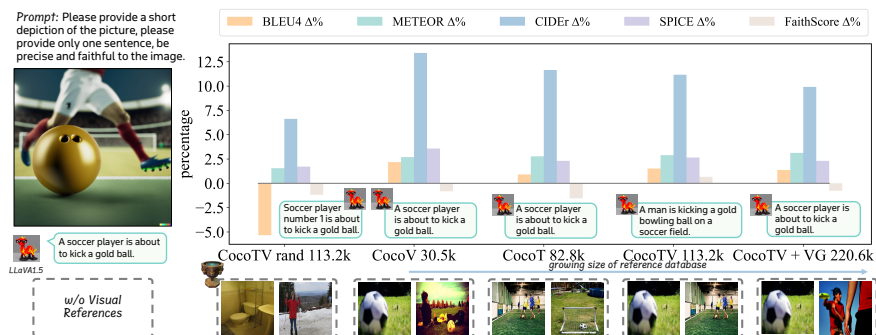


Fig. 5: A reference database containing 113k reference images from COCO Caption Karpathy *train* (T) and *restval* (V) splits can improve performance across all metrics, to address potential noisy retrieval results. Overall, the performance gain positively correlates with the similarity between the test image and the references. The baseline (depicted as the grey horizontal line) is Exp.1 in Tab. 4. *rand* denotes sampling random references (Exp.3).

We provide qualitative evidences in Fig. 2 and in Appendix D to support this hypothesis. For quantitative analysis, we randomly select 200 images from the OpenImages [24] validation set and generate a one-sentence caption for each sample using LLaVA1.5-7B. We manually review the confidence scores within the head vocabulary of each generated token in all generated captions, and find that 18 captions contain at least one hallucinatory token. Notably, 10 out of these 18 erroneous captions exhibit analogous visual hallucinations across similar images. We expect detailed candidate-level visual hallucination annotations and automatic evaluation pipelines to be developed in the future. Nonetheless, our observation in Sec. 3.2 demonstrates that analogous visual hallucinations can be leveraged to mitigate hallucination.

Pensieve introduces $\mathcal{O}(k)$ time complexity, as distinct confidence scores are independently predicted for each visual reference. This latency can be reduced by predicting reference confidence scores in parallel. Note that we save a significant amount of time and human labor required for data curation and model training.

7 Conclusion

We address the issue of visual hallucinations in MLLMs. Through a comprehensive analysis, we discover that analogous visual hallucinations induced by similar images can be utilized to reduce hallucination. Building on this insight, we introduce *Pensieve*, a training-free method that allows MLLMs to retrospect similar images as references and discern the accurate visual cues through confidence score comparison. This paradigm corrects the erroneous content that is mistakenly supported by MLLMs’ visual or textual branches. Quantitative and qualitative experiments on image captioning and VQA benchmarks demonstrate the superiority of *Pensieve* over other advanced decoding strategies.

Acknowledgment: This work is supported by the National Natural Science Foundation of China (No. 62372329), in part by the National Key Research and Development Program of China (No. 2021YFB2501104), in part by Shanghai Rising Star Program (No.21QC1400900), in part by Tongji-Qomolo Autonomous Driving Commercial Vehicle Joint Lab Project, and in part by Xiaomi Young Talents Program. We would like to acknowledge the discussions and comments for this project from Zehan Zheng.

References

1. An, W., Tian, F., Leng, S., Nie, J., Lin, H., Wang, Q., Dai, G., Chen, P., Lu, S.: Apla: Mitigating object hallucinations in large vision-language models with assembly of global and local attention. arXiv preprint arXiv:2406.12718 (2024) [4](#)
2. Anderson, P., Fernando, B., Johnson, M., Gould, S.: Spice: Semantic propositional image caption evaluation. In: Computer Vision—ECCV 2016: 14th European Conference, Amsterdam, The Netherlands, October 11–14, 2016, Proceedings, Part V 14. pp. 382–398. Springer (2016) [10](#)
3. Bitton-Guetta, N., Bitton, Y., Hessel, J., Schmidt, L., Elovici, Y., Stanovsky, G., Schwartz, R.: Breaking common sense: Whoops! a vision-and-language benchmark of synthetic and compositional images. In: Proceedings of the IEEE/CVF International Conference on Computer Vision. pp. 2616–2627 (2023) [3](#), [9](#), [23](#)
4. Chen, B., Lyu, X., Gao, L., Song, J., Shen, H.T.: Alleviating hallucinations in large vision-language models through hallucination-induced optimization. arXiv preprint arXiv:2405.15356 (2024) [1](#)
5. Chen, B., Lyu, X., Gao, L., Song, J., Shen, H.T.: Alleviating hallucinations in large vision-language models through hallucination-induced optimization. arXiv preprint arXiv:2405.15356 (2024) [4](#)
6. Chen, K., Zhang, Z., Zeng, W., Zhang, R., Zhu, F., Zhao, R.: Shikra: Unleashing multimodal llm’s referential dialogue magic. arXiv preprint arXiv:2306.15195 (2023) [1](#), [5](#)
7. Chen, L., Li, J., Dong, X., Zhang, P., He, C., Wang, J., Zhao, F., Lin, D.: Sharegpt4v: Improving large multi-modal models with better captions. arXiv preprint arXiv:2311.12793 (2023) [21](#)
8. Chen, Z., Zhao, Z., Luo, H., Yao, H., Li, B., Zhou, J.: Halc: Object hallucination reduction via adaptive focal-contrast decoding. arXiv preprint arXiv:2403.00425 (2024) [4](#)
9. Chen, Z., Zhu, Y., Zhan, Y., Li, Z., Zhao, C., Wang, J., Tang, M.: Mitigating hallucination in visual language models with visual supervision. arXiv preprint arXiv:2311.16479 (2023) [1](#), [3](#), [4](#)
10. Chuang, Y.S., Xie, Y., Luo, H., Kim, Y., Glass, J., He, P.: Dola: Decoding by contrasting layers improves factuality in large language models. arXiv preprint arXiv:2309.03883 (2023) [9](#)
11. Dai, W., Li, J., Li, D., Tiong, A.M.H., Zhao, J., Wang, W., Li, B., Fung, P., Hoi, S.: Instructblip: Towards general-purpose vision-language models with instruction tuning (2023) [1](#), [3](#), [5](#), [7](#), [9](#), [10](#), [23](#)
12. Denkowski, M., Lavie, A.: Meteor universal: Language specific translation evaluation for any target language. In: Proceedings of the ninth workshop on statistical machine translation. pp. 376–380 (2014) [10](#)

13. Dosovitskiy, A., Beyer, L., Kolesnikov, A., Weissenborn, D., Zhai, X., Unterthiner, T., Dehghani, M., Minderer, M., Heigold, G., Gelly, S., et al.: An image is worth 16x16 words: Transformers for image recognition at scale. arXiv preprint arXiv:2010.11929 (2020) [22](#)
14. Douze, M., Guzhva, A., Deng, C., Johnson, J., Szilvassy, G., Mazaré, P.E., Lomeli, M., Hosseini, L., Jégou, H.: The faiss library (2024) [22](#)
15. Favero, A., Zancato, L., Trager, M., Choudhary, S., Perera, P., Achille, A., Swaminathan, A., Soatto, S.: Multi-modal hallucination control by visual information grounding. In: Proceedings of the IEEE/CVF Conference on Computer Vision and Pattern Recognition. pp. 14303–14312 (2024) [2](#), [4](#)
16. Fu, C., Chen, P., Shen, Y., Qin, Y., Zhang, M., Lin, X., Yang, J., Zheng, X., Li, K., Sun, X., et al.: Mme: A comprehensive evaluation benchmark for multimodal large language models. arXiv preprint arXiv:2306.13394 (2023) [3](#), [9](#), [23](#)
17. Hessel, J., Holtzman, A., Forbes, M., Bras, R.L., Choi, Y.: Clipscore: A reference-free evaluation metric for image captioning. arXiv preprint arXiv:2104.08718 (2021) [23](#)
18. Ho, J., Jain, A., Abbeel, P.: Denoising diffusion probabilistic models. Advances in neural information processing systems **33**, 6840–6851 (2020) [6](#), [21](#)
19. Huang, Q., Dong, X., Zhang, P., Wang, B., He, C., Wang, J., Lin, D., Zhang, W., Yu, N.: Opera: Alleviating hallucination in multi-modal large language models via over-trust penalty and retrospection-allocation. arXiv preprint arXiv:2311.17911 (2023) [1](#), [2](#), [3](#), [4](#)
20. Jiang, C., Xu, H., Dong, M., Chen, J., Ye, W., Yan, M., Ye, Q., Zhang, J., Huang, F., Zhang, S.: Hallucination augmented contrastive learning for multimodal large language model. arXiv preprint arXiv:2312.06968 (2023) [1](#), [2](#), [3](#), [4](#)
21. Jing, L., Li, R., Chen, Y., Jia, M., Du, X.: Faithscore: Evaluating hallucinations in large vision-language models. arXiv preprint arXiv:2311.01477 (2023) [1](#), [3](#), [10](#), [23](#)
22. Karpathy, A., Fei-Fei, L.: Deep visual-semantic alignments for generating image descriptions. In: Proceedings of the IEEE conference on computer vision and pattern recognition. pp. 3128–3137 (2015) [7](#)
23. Krishna, R., Zhu, Y., Groth, O., Johnson, J., Hata, K., Kravitz, J., Chen, S., Kalantidis, Y., Li, L.J., Shamma, D.A., et al.: Visual genome: Connecting language and vision using crowdsourced dense image annotations. International journal of computer vision **123**, 32–73 (2017) [13](#), [21](#), [24](#)
24. Kuznetsova, A., Rom, H., Alldrin, N., Uijlings, J., Krasin, I., Pont-Tuset, J., Kamali, S., Popov, S., Mallocci, M., Kolesnikov, A., et al.: The open images dataset v4: Unified image classification, object detection, and visual relationship detection at scale. International journal of computer vision **128**(7), 1956–1981 (2020) [5](#), [14](#), [29](#)
25. Lee, N., Ping, W., Xu, P., Patwary, M., Fung, P.N., Shoeybi, M., Catanzaro, B.: Factuality enhanced language models for open-ended text generation. Advances in Neural Information Processing Systems **35**, 34586–34599 (2022) [9](#)
26. Lee, S., Park, S.H., Jo, Y., Seo, M.: Volcano: mitigating multimodal hallucination through self-feedback guided revision. arXiv preprint arXiv:2311.07362 (2023) [2](#), [3](#)
27. Leng, S., Zhang, H., Chen, G., Li, X., Lu, S., Miao, C., Bing, L.: Mitigating object hallucinations in large vision-language models through visual contrastive decoding. arXiv preprint arXiv:2311.16922 (2023) [1](#), [2](#), [3](#), [4](#), [6](#), [9](#), [11](#)
28. Li, J., Vo, D.M., Sugimoto, A., Nakayama, H.: Evcap: Retrieval-augmented image captioning with external visual-name memory for open-world comprehension. arXiv preprint arXiv:2311.15879 (2023) [10](#)

29. Li, J., Li, D., Savarese, S., Hoi, S.: Blip-2: Bootstrapping language-image pre-training with frozen image encoders and large language models. arXiv preprint arXiv:2301.12597 (2023) [1](#), [23](#)
30. Li, J., Chen, J., Ren, R., Cheng, X., Zhao, W.X., Nie, J.Y., Wen, J.R.: The dawn after the dark: An empirical study on factuality hallucination in large language models. arXiv preprint arXiv:2401.03205 (2024) [9](#)
31. Li, X.L., Holtzman, A., Fried, D., Liang, P., Eisner, J., Hashimoto, T., Zettlemoyer, L., Lewis, M.: Contrastive decoding: Open-ended text generation as optimization. arXiv preprint arXiv:2210.15097 (2022) [4](#), [9](#)
32. Li, Y., Du, Y., Zhou, K., Wang, J., Zhao, W.X., Wen, J.R.: Evaluating object hallucination in large vision-language models. arXiv preprint arXiv:2305.10355 (2023) [3](#), [9](#), [23](#)
33. Lin, B.Y., Ravichander, A., Lu, X., Dziri, N., Sclar, M., Chandu, K., Bhagavatula, C., Choi, Y.: The unlocking spell on base llms: Rethinking alignment via in-context learning. arXiv preprint arXiv:2312.01552 (2023) [6](#)
34. Lin, T.Y., Maire, M., Belongie, S., Hays, J., Perona, P., Ramanan, D., Dollár, P., Zitnick, C.L.: Microsoft coco: Common objects in context. In: Computer Vision—ECCV 2014: 13th European Conference, Zurich, Switzerland, September 6–12, 2014, Proceedings, Part V 13. pp. 740–755. Springer (2014) [7](#), [21](#)
35. Lin, Z., Liu, C., Zhang, R., Gao, P., Qiu, L., Xiao, H., Qiu, H., Lin, C., Shao, W., Chen, K., et al.: Sphinx: The joint mixing of weights, tasks, and visual embeddings for multi-modal large language models. arXiv preprint arXiv:2311.07575 (2023) [1](#), [5](#)
36. Liu, F., Lin, K., Li, L., Wang, J., Yacoob, Y., Wang, L.: Mitigating hallucination in large multi-modal models via robust instruction tuning. arXiv preprint arXiv:2306.14565 **1**(2), [9](#) (2023) [1](#), [3](#), [4](#)
37. Liu, H., Xue, W., Chen, Y., Chen, D., Zhao, X., Wang, K., Hou, L., Li, R., Peng, W.: A survey on hallucination in large vision-language models. arXiv preprint arXiv:2402.00253 (2024) [1](#), [3](#)
38. Liu, H., Li, C., Li, Y., Lee, Y.J.: Improved baselines with visual instruction tuning (2023) [1](#), [3](#), [5](#), [6](#), [7](#), [9](#), [10](#), [21](#), [23](#)
39. Liu, H., Li, C., Wu, Q., Lee, Y.J.: Visual instruction tuning. *Advances in neural information processing systems* **36** (2024) [3](#), [9](#), [10](#), [23](#), [38](#)
40. Liu, J., Fu, Y., Xie, R., Xie, R., Sun, X., Lian, F., Kang, Z., Li, X.: Phd: A prompted visual hallucination evaluation dataset. arXiv preprint arXiv:2403.11116 (2024) [3](#)
41. Oquab, M., Darcet, T., Moutakanni, T., Vo, H., Szafraniec, M., Khalidov, V., Fernandez, P., Haziza, D., Massa, F., El-Nouby, A., et al.: Dinov2: Learning robust visual features without supervision. arXiv preprint arXiv:2304.07193 (2023) [22](#)
42. Papineni, K., Roukos, S., Ward, T., Zhu, W.J.: Bleu: a method for automatic evaluation of machine translation. In: Proceedings of the 40th annual meeting of the Association for Computational Linguistics. pp. 311–318 (2002) [10](#), [22](#)
43. Radford, A., Kim, J.W., Hallacy, C., Ramesh, A., Goh, G., Agarwal, S., Sastry, G., Askell, A., Mishkin, P., Clark, J., et al.: Learning transferable visual models from natural language supervision. In: International conference on machine learning. pp. 8748–8763. PMLR (2021) [22](#)
44. Rohrbach, A., Hendricks, L.A., Burns, K., Darrell, T., Saenko, K.: Object hallucination in image captioning. arXiv preprint arXiv:1809.02156 (2018) [3](#), [23](#)
45. Shi, W., Han, X., Lewis, M., Tsvetkov, Y., Zettlemoyer, L., Yih, S.W.t.: Trusting your evidence: Hallucinate less with context-aware decoding. arXiv preprint arXiv:2305.14739 (2023) [3](#)

46. Sun, Z., Shen, S., Cao, S., Liu, H., Li, C., Shen, Y., Gan, C., Gui, L.Y., Wang, Y.X., Yang, Y., et al.: Aligning large multimodal models with factually augmented rlhf. arXiv preprint arXiv:2309.14525 (2023) [1](#), [2](#), [4](#)
47. Tong, S., Brown, E., Wu, P., Woo, S., Middepogu, M., Akula, S.C., Yang, J., Yang, S., Iyer, A., Pan, X., et al.: Cambrian-1: A fully open, vision-centric exploration of multimodal llms. arXiv preprint arXiv:2406.16860 (2024) [1](#)
48. Tong, S., Liu, Z., Zhai, Y., Ma, Y., LeCun, Y., Xie, S.: Eyes wide shut? exploring the visual shortcomings of multimodal llms. arXiv preprint arXiv:2401.06209 (2024) [1](#), [2](#), [3](#), [22](#)
49. Touvron, H., Martin, L., Stone, K., Albert, P., Almahairi, A., Babaei, Y., Bashlykov, N., Batra, S., Bhargava, P., Bhosale, S., et al.: Llama 2: Open foundation and fine-tuned chat models. arXiv preprint arXiv:2307.09288 (2023) [5](#)
50. Vaswani, A., Shazeer, N., Parmar, N., Uszkoreit, J., Jones, L., Gomez, A.N., Kaiser, Ł., Polosukhin, I.: Attention is all you need. *Advances in neural information processing systems* **30** (2017) [22](#)
51. Vedantam, R., Lawrence Zitnick, C., Parikh, D.: Cider: Consensus-based image description evaluation. In: *Proceedings of the IEEE conference on computer vision and pattern recognition*. pp. 4566–4575 (2015) [10](#)
52. Wang, J., Wang, Y., Xu, G., Zhang, J., Gu, Y., Jia, H., Yan, M., Zhang, J., Sang, J.: An llm-free multi-dimensional benchmark for mllms hallucination evaluation. arXiv preprint arXiv:2311.07397 (2023) [3](#)
53. Wang, J., Zhou, Y., Xu, G., Shi, P., Zhao, C., Xu, H., Ye, Q., Yan, M., Zhang, J., Zhu, J., et al.: Evaluation and analysis of hallucination in large vision-language models. arXiv preprint arXiv:2308.15126 (2023) [1](#), [2](#), [3](#), [9](#)
54. Wang, P., Yang, A., Men, R., Lin, J., Bai, S., Li, Z., Ma, J., Zhou, C., Zhou, J., Yang, H.: Ofa: Unifying architectures, tasks, and modalities through a simple sequence-to-sequence learning framework. *CoRR* **abs/2202.03052** (2022) [10](#), [23](#)
55. Wang, X., Pan, J., Ding, L., Biemann, C.: Mitigating hallucinations in large vision-language models with instruction contrastive decoding. arXiv preprint arXiv:2403.18715 (2024) [4](#)
56. Wang, X., Zhou, Y., Liu, X., Lu, H., Xu, Y., He, F., Yoon, J., Lu, T., Bertasius, G., Bansal, M., et al.: Mementos: A comprehensive benchmark for multimodal large language model reasoning over image sequences. arXiv preprint arXiv:2401.10529 (2024) [3](#)
57. Wu, K., Jiang, B., Jiang, Z., He, Q., Luo, D., Wang, S., Liu, Q., Wang, C.: Noise-boost: Alleviating hallucination with noise perturbation for multimodal large language models. arXiv preprint arXiv:2405.20081 (2024) [3](#)
58. Wu, M., Ji, J., Huang, O., Li, J., Wu, Y., Sun, X., Ji, R.: Evaluating and analyzing relationship hallucinations in large vision-language models. In: *Forty-first International Conference on Machine Learning* (2024) [3](#)
59. Xie, N., Lai, F., Doran, D., Kadav, A.: Visual entailment: A novel task for fine-grained image understanding. arXiv preprint arXiv:1901.06706 (2019) [23](#)
60. Yan, B., Zhang, J., Yuan, Z., Shan, S., Chen, X.: Evaluating the quality of hallucination benchmarks for large vision-language models. arXiv preprint arXiv:2406.17115 (2024) [1](#)
61. Yin, S., Fu, C., Zhao, S., Xu, T., Wang, H., Sui, D., Shen, Y., Li, K., Sun, X., Chen, E.: Woodpecker: Hallucination correction for multimodal large language models. arXiv preprint arXiv:2310.16045 (2023) [1](#), [4](#), [11](#)
62. You, H., Zhang, H., Gan, Z., Du, X., Zhang, B., Wang, Z., Cao, L., Chang, S.F., Yang, Y.: Ferret: Refer and ground anything anywhere at any granularity. arXiv preprint arXiv:2310.07704 (2023) [1](#), [5](#)

63. Yu, T., Zhang, H., Yao, Y., Dang, Y., Chen, D., Lu, X., Cui, G., He, T., Liu, Z., Chua, T.S., et al.: Rlaif-v: Aligning mllms through open-source ai feedback for super gpt-4v trustworthiness. arXiv preprint arXiv:2405.17220 (2024) [4](#)
64. Yuan, Y., Li, W., Liu, J., Tang, D., Luo, X., Qin, C., Zhang, L., Zhu, J.: Osprey: Pixel understanding with visual instruction tuning. arXiv preprint arXiv:2312.10032 (2023) [1](#)
65. Yue, Z., Zhang, L., Jin, Q.: Less is more: Mitigating multimodal hallucination from an eos decision perspective. arXiv preprint arXiv:2402.14545 (2024) [3](#)
66. Zhai, B., Yang, S., Zhao, X., Xu, C., Shen, S., Zhao, D., Keutzer, K., Li, M., Yan, T., Fan, X.: Halle-switch: Rethinking and controlling object existence hallucinations in large vision language models for detailed caption. arXiv preprint arXiv:2310.01779 (2023) [3](#)
67. Zhang, H., Zhang, J., Wan, X.: Evaluating and mitigating number hallucinations in large vision-language models: A consistency perspective. arXiv preprint arXiv:2403.01373 (2024) [3](#)
68. Zhang, M., Press, O., Merrill, W., Liu, A., Smith, N.A.: How language model hallucinations can snowball. arXiv preprint arXiv:2305.13534 (2023) [3](#)
69. Zhang, P., Dong, X., Zang, Y., Cao, Y., Qian, R., Chen, L., Guo, Q., Duan, H., Wang, B., Ouyang, L., et al.: Internlm-xcomposer-2.5: A versatile large vision language model supporting long-contextual input and output. arXiv preprint arXiv:2407.03320 (2024) [1](#)
70. Zhang, S., Sun, P., Chen, S., Xiao, M., Shao, W., Zhang, W., Chen, K., Luo, P.: Gpt4roi: Instruction tuning large language model on region-of-interest. arXiv preprint arXiv:2307.03601 (2023) [1](#)
71. Zhang, Y.F., Yu, W., Wen, Q., Wang, X., Zhang, Z., Wang, L., Jin, R., Tan, T.: Debiasing large visual language models. arXiv preprint arXiv:2403.05262 (2024) [2](#), [4](#)
72. Zhao, L., Deng, Y., Zhang, W., Gu, Q.: Mitigating object hallucination in large vision-language models via classifier-free guidance. arXiv preprint arXiv:2402.08680 (2024) [4](#)
73. Zhao, Z., Wallace, E., Feng, S., Klein, D., Singh, S.: Calibrate before use: Improving few-shot performance of language models. In: International Conference on Machine Learning. pp. 12697–12706. PMLR (2021) [4](#)
74. Zheng, L., Chiang, W.L., Sheng, Y., Zhuang, S., Wu, Z., Zhuang, Y., Lin, Z., Li, Z., Li, D., Xing, E.P., Zhang, H., Gonzalez, J.E., Stoica, I.: Judging llm-as-a-judge with mt-bench and chatbot arena (2023) [5](#), [9](#), [20](#), [23](#)
75. Zhou, Y., Cui, C., Yoon, J., Zhang, L., Deng, Z., Finn, C., Bansal, M., Yao, H.: Analyzing and mitigating object hallucination in large vision-language models. arXiv preprint arXiv:2310.00754 (2023) [1](#), [2](#), [3](#), [4](#), [9](#)
76. Zhu, D., Chen, J., Shen, X., Li, X., Elhoseiny, M.: Minigt-4: Enhancing vision-language understanding with advanced large language models. arXiv preprint arXiv:2304.10592 (2023) [1](#), [5](#)

A Explanations for our Analysis Pipeline

A.1 Semantics in MLLMs’ Last Hidden State

We term $E_c(x_i)$ the token embedding of candidate x_i in the language head⁸, where $E_c(\cdot)$ embeds token x_i into a feature vector with hidden dimension d . The feature vectors of all candidates (the total number is the length of the model’s vocabulary $length(\mathcal{V})$) forms the weight matrix in the language head with the shape of $[length(\mathcal{V}), d]$. Since the language head is a linear projection layer without dropout, activate function, or bias, the confidence score at decoding step t corresponding to candidate x_i is the inner product of its embedding $E_c(x_i)$ and the last hidden state \mathbf{h}_t predicted by the MLLMs’ final attention block. If the confidence scores of different candidates are close, then \mathbf{h}_t is a blend of diverse semantics in near proportions. Subsequently, those close confidence scores will result in low probabilities after the softmax operator, indicating that MLLMs are *unsure* about their current prediction.

Following our proposed analysis pipeline, if the score shift $\Delta\mathbf{h} \cdot E_c(x_i)$ corresponding to candidate x_i is a positive value, then $\Delta\mathbf{h}$ strengthens the semantics corresponding to x_i . On the other hand, some semantics can be weakened by $\Delta\mathbf{h}$, if the candidates get negative *img score*. If the score shift is close to zero, we claim $\Delta\mathbf{h}$ is orthogonal to $E_c(x_i)$.

A.2 Quantify MLLMs’ Blindness

We use the Jensen-Shannon Divergence (JSD) to help quantify the extent of dependency of MLLMs’ predictions on the visual input. Specifically, JSD is calculated between the confidence scores predicted by the test image \mathbf{v}^τ and the diffused image \mathbf{v}^d in the same context $\mathbf{x} + \mathbf{y}_{<t}$, within the head vocabulary \mathcal{V}_{head}^m of m top-ranked candidates. Formally,

$$\text{JSD}(P \parallel Q) = \frac{1}{2} (D_{KL}(P \parallel M) + D_{KL}(Q \parallel M)) \quad (9)$$

$$M = \frac{1}{2} (P + Q) \quad (10)$$

$$P = \text{softmax}(\{\text{logits}(x_j | \mathbf{x}, \mathbf{y}_{<t}, \mathbf{v}^\tau) | x_j \in \mathcal{V}_{head}^m\}) \quad (11)$$

$$Q = \text{softmax}(\{\text{logits}(x_j | \mathbf{x}, \mathbf{y}_{<t}, \mathbf{v}^d) | x_j \in \mathcal{V}_{head}^m\}) \quad (12)$$

where $D_{KL}(\cdot)$ is the KL divergence. A high JSD value suggests that the *base scores* and the *txt scores* will yield different probability distributions following the softmax operator. Therefore, the subtraction of the of *txt scores* from the *base scores* (*i.e.*, the *img scores*) will *not* be uniformly distributed, indicating

⁸ The parameters in the language head of Vicuna [74] is not tied to its input token embedding layer.

that some (but not all) candidates are advocated by the visual branch. On the contrary, if both the JSD and the first place candidate’s *img score* (denoted as the *top-1 img score*) are close to zero, then the visual information **hardly** impacts the prediction, *i.e.*, contributes few probabilities to token candidates at the current decoding step. From the examples in Fig. 2 and in Appendix D (Fig. 9 to Fig. 12), we notice that in a sentence, the JSD values corresponding to erroneous tokens in the sentence are **not** close to zero. This manifests that MLLMs is **not** utterly ignorant of the visual cues in the image amidst visual hallucination.

B Implementation Details

B.1 Details for the Diffusion Process.

We implement the diffusion process [18] to erase visual information in the test image. This process involves gradually adding noise to an initial image x_0 until it becomes pure Gaussian noise x_T . At a specific step $t \in [0, T]$, a small amount of noise is added to the image from the previous step $t - 1$. Formally,

$$x_t = \sqrt{\alpha_t}x_{t-1} + \sqrt{1 - \alpha_t}\epsilon_t \quad (13)$$

where α_t is a parameter that controls the amount of noise added at each step. The parameters $\{\alpha_t\}_{t=1}^T$ are chosen such that they form a schedule, typically decreasing over t . ϵ_t is Gaussian noise sampled from a normal distribution $\mathcal{N}(0, I)$, where I is the identity matrix. Equation 13 is iterated for a number of steps T . To obtain x_t directly from x_0 in the forward diffusion process without iterating through each intermediate step, Equation 14 can be derived, which encapsulates the cumulative effect of adding noise over multiple steps,

$$x_t = \sqrt{\bar{\alpha}_t}x_0 + \sqrt{1 - \bar{\alpha}_t}\epsilon \quad (14)$$

where $\bar{\alpha}_t = \prod_{i=1}^t \alpha_i$ is the cumulative product of the noise schedule parameters up to step t . ϵ is Gaussian noise sampled from a normal distribution $\mathcal{N}(0, I)$. We present a diffused image ($t = 999$) in Fig. 2, which scarcely retains any valid visual information and is nearly indistinguishable from Gaussian noise.

B.2 Details for Visual Retrospection

Reference Database. We build our reference database with the COCO Caption [34] dataset, which is the basis for popular visual instruction datasets [7, 38]. We expect the visual references to be capable of **inducing** visual hallucinations, such that the analogous hallucinations can be further leveraged to reduce hallucination. Additionally, images in COCO Caption contain daily and common visual concepts, such that they are less likely to induce out-of-distribution and confusing responses. We also include the Visual Genome dataset [23] to enlarge the database, but the performance gain is lower than utilizing COCO-Caption only (see Sec. 5.3).

Retrievers. For image captioning, the retriever extracts semantic and appearance features from the visual inputs \mathbf{v} into $E_R(\mathbf{v})$. The CLIP [43] vision transformer [13] is adept at encoding semantics, and the self-supervised pretrained DINOv2 [41] ViT can capture more visual details [48]. We ensemble CLIP and DINOv2 ViT-L14/336 model as the image retriever. For Visual Question Answering (VQA), The CLIP Transformer [50] extract semantics from the question \mathbf{x} into a vector embedding $E_R(\mathbf{x})$. We target at finding visual references that are semantically accordant to the question. Note that we do not add visual representations here because they may perturb the semantics in $E_R(\mathbf{x})$. Before text encoding, we modify the question template in MME and POPE to transform questions into narratives, *e.g.*, replacing *Is there* with *A photo of*.

Similarity Metrics. $\mathcal{F}(\cdot, \cdot)$ is the cosine similarity. Specifically, representations are L2 normalized before the Maximum Inner Product Search (MIPS) conducted by FAISS [14], which is a library for vector clustering and similarity search. For image captioning, we concatenate the *[cls]* token from CLIP and DINOv2 Vision Transformer models. Therefore, the semantic and appearance similarities are equally considered. For VQA on the MME benchmark, we further re-order the retrieval results based on the BLEU@1 [42] score between the search query and the captions of retrieved images.

B.3 Details for Visual Comparison

If not otherwise specified, we refer the rank to the ranking of candidates according to the *base scores* predicted by the test image \mathbf{v}^T . At decoding step t , we set a cut-off value as the m^{th} -ranked candidate’s *base score*. The confidence scores lower than this threshold are set to *-inf*. Therefore, the candidates outside the head vocabulary \mathcal{V}_{head}^m will not be considered during token selection.

In the adaptive logits processing method (Eq. (6) to Eq. (8)) the lower bound of the maximum probability after the softmax operator is $1/50 = 0.02$, if all candidates within \mathcal{V}_{head}^m have exactly the same confidence scores. This scheme is designed to reduce potential erroneous support from the diffused image \mathbf{v}^d to the erroneous candidates, especially the visually deceptive candidates, when \mathbf{v}^d tends to equally support multiple candidates at decoding step t .

Compare when Necessary. We observe that the JSD value can be very close to zero at some decoding steps, especially in subwords and lexical collocation, such as *ing* after *_lay* in Fig. 9, and *ck* after *_du* in Fig. 12. Modifying their confidence score distribution may harm language fluency and induce grammatical errors. Therefore, we optionally set a JSD threshold to disable *Pensieve* at certain decoding steps (although we do not use it in practice for image captioning in all reported quantitative experiments).

C Experiments

C.1 Detailed Experimental Settings

Datasets and Metrics. We use POPE (the Polling-based Object Probing Evaluation [32]), the Count and Existence subtasks of MME [16] for object-level visual hallucination evaluation. The Color and Position subtasks of MME assess the attribute-level hallucination. On these benchmarks, The MLLMs are explicitly prompted to answer yes or no. Based on whether the response contains the string *yes* or *no*, the Accuracy, Precision, Recall, and F1 score are determined on POPE, and the Accuracy and Accuracy+ are combined on MME as the official evaluation metrics, respectively.

Considering that the performance in binary VQA task may not be able to capture the extent of visual hallucination in free-form text generation process, we further evaluate our proposed *Pensieve* on two challenging benchmarks. The Whoops [3] benchmark contains 500 generated high-fidelity images with some of the visual cues violating common sense. LLaVA Bench in the Wild [39](abbreviated as $LLaVA^W$) contains 60 questions on 24 images, including indoor and outdoor scenes, memes, paintings, and sketches.

For visual hallucination evaluation on Whoops and $LLaVA^W$, we use the FaithScore [21] metric, which is adept at judging the extent of visual hallucinations at a finer granularity (beyond object and attribute-level errors), and shows a higher correlation with human judgment than traditional metrics like CHAIR [44] and CLIP-Score [17]. Specifically, We prompt ChatGPT (the *gpt-3.5-turbo-1106* API⁹) to identify descriptive sentences in the response, and extract atomic facts from those sentences. For atomic facts verification, we use the recommended model OFA [54], instead of a model from the LLaVA or BLIP family, as we are evaluating LLaVA-1.5-7B and InstructBLIP-7B. OFA is finetuned on the visual entailment dataset SNLI-VE [59], showing comparable performance as LLaVA-1.5 on atomic fact verification [21]. The FaithScore is adept at indicating the comprehensive degree of visual hallucination. For all experiments, we query ChatGPT three times and report the averaged results.

Hyper-parameters are detailed in Tab. 5. Note that for InstructBLIP on the POPE-GQA subset only, the hyper-parameters are set to $\alpha_\tau = 1.0$, $\beta_d = 0.1$, $\beta_{NN} = 0.1$ for better performance.

MLLM Baselines. We select two representative open-source MLLMs [11, 38] to implement our method. Both MLLMs integrate CLIP Vision Transformer as the visual encoder. As for the cross-modal connector, LLaVA-1.5 uses a two-layer MLP, and InstructBLIP uses a Q-former [29] with textual input. We use the 7B version of both MLLMs, with Vicuna-7B [74] as the language decoder.

⁹ <https://openai.com/blog/chatgpt>

Model	Hyper-param.	Whoops	LLaVA ^W	MME	POPE
LLaVA-1.5	k	4	2	1	2
	β_{NN}	0.1	0.1	0.01	0.05
	β_d	0.1	0.1	0.1	0.01
	α_r	1.0	1.0	1.0	1.0
	diffu. step	900	900	700	900
InstructBLIP	k	2	2	2	2
	β_{NN}	0.04	0.1	0.1	0.02
	β_d	0.05	0.1	0.5	0.02
	α_r	1.2	1.0	1.0	1.5
	diffu. step	500	900	900	900

Table 5: Detailed hyper-parameter setting for LLaVA-1.5 and InstructBLIP for each test dataset. diffu. step denotes the image diffusion step.

Settings for the Ablation Study. For all ablation studies, we use LLaVA-1.5-7B as the baseline MLLM, and the default hyper-parameter setting (the same as the experiment on Whoops). In ablation study Exp.3, we retrieve five sets of random visual references for each test sample, and report the averaged results on five separate runs. In Exp.4, we set $\beta_d = 1e - 6$ to discard the impact of the diffused image \mathbf{v}^d on confidence score modification. We do not discard the diffused image itself, since we still need it to calculate α_d^t and α_{NN}^t . In Exp.6, we fix both α_d^t and α_{NN}^t to 0.1. In the study of the reference database size, we include all images (108k) from the Visual Genome [23] dataset.

C.2 More Results on LLaVA Bench in the Wild

We present more qualitative results to demonstrate the superiority of our proposed *Pensieve*. Figures 6 and 7 demonstrate that *Pensieve* helps LLaVA1.5 and InstructBLIP correctly describe challenging scenes, which contain visual cues that are difficult to distinguish. Specifically, *Pensieve* helps LLaVA1.5 correctly identify the small buildings scattered around the large antenna, and helps InstructBLIP discern the streetlights from traffic lights near the highway. *Pensieve* also successfully corrects visual hallucinations that confuse both DoLa and VCD such as the dining table, the bananas, and the man ironing on the roof of a car. Additionally, *Pensieve* is capable of correcting erroneous nouns, adjectives, prepositions, *etc.*, wherever they appear in the sentence.

In summary, *Pensieve* generalizes well on various image domains, including photographs, paintings, and text-rich images. Moreover, *Pensieve* is a versatile method that is adept at mitigating various hallucination categories, **NOT** limited to pre-defined error types.

C.3 More Results on MME

Quantitative Results. We present results on all perception tasks of MME in Tab. 6. Note that we concentrate on the problem of visual hallucination, facilitating MLLMs to faithfully describe the image. The cognition tasks that



Fig. 6: More qualitative results on LLaVA-Bench in the wild. Our proposed *Pensieve* effectively reduces visual hallucination for LLaVA1.5-7B. Retrieved visual references are in the grey box. Hallucinatory content is marked in red.

necessitate specified knowledge (commonsense reasoning, numerical calculation, text translation, and code reasoning) is beyond the scope of this work. Table 6 demonstrate that our proposed *Pensieve* improves the overall perception performance for both MLLMs, increasing the total score for LLaVA1.5 by 56.6, and the total score for InstructBLIP by 76.3, outperforming other advanced decoding strategies.

Table 6: Results on all perception sub-tasks of the MME benchmark. We report the officially defined metric that combines Accuracy and Accuracy+. *Pensieve* substantially improves the perception competencies for both MLLMs.

Model	Decoding	Color ↑	Count ↑	Existence ↑	Position ↑	Posters ↑	Celebrity ↑	Scene ↑	Landmark ↑	Artwork ↑	OCR ↑	Total ↑
LLaVA-1.5	greedy	155.0	158.3	195.0	123.3	129.6	132.6	155.0	163.5	121.0	125.0	1458.9
	+DoLa	153.3	158.3	195.0	123.3	127.6	130.9	154.8	162.8	122.3	122.5	1450.7
	+VCD	148.3	158.3	190.0	126.7	136.7	147.4	148.8	166.0	122.5	130.0	1474.7
	+Ours	165.0	153.3	195.0	128.3	141.8	150.3	157.3	161.8	122.8	140.0	1515.5
	greedy	120.0	60.0	185.0	50.0	142.9	81.8	160.0	160.0	92.0	65.0	1116.6
InstructBLIP	+DoLa	120.0	60.0	185.0	50.0	142.9	80.9	160.0	160.0	92.2	65.0	1116.0
	+VCD	123.3	60.0	185.0	53.3	151.7	94.1	156.5	161.3	99.3	95.0	1179.5
	+Ours	153.3	78.3	180.0	58.3	140.5	71.2	163.8	158.3	94.3	95.0	1192.9

Case Study. We investigate how *Pensieve* enhances model performance on the MME benchmark and present the results in Fig. 8. We plot the confidence scores



Fig. 7: More qualitative results on LLaVA-Bench in the wild. Our proposed *Pensieve* effectively reduces visual hallucination for InstructBLIP-7B. Retrieved visual references are in the grey box. Hallucinatory content is marked in red.

corresponding to the candidates *_yes* and *_no* on the vertical and horizontal axis, respectively. Each test sample corresponds to a single triangle mark colored in blue (the samples' ground truth answer is *_yes*) or red (the ground truth answer is *_no*). If a blue triangle mark is below the $y = x$ line, or a red triangle mark is above the $y = x$ line, then the answer is incorrect. We summarize our main observations as follows:

- Without visual references, the scores of the two candidates can be close. As illustrated in the first row in Fig. 8, a number of predicted samples in the Count and Position task are close to the $y = x$ line. This indicates LLaVA1.5 has equal confidence, *i.e.*, high perplexity, to the positive and negative answers.
- InstructBLIP tends to answer yes for all provided questions, regardless of their ground truth label. As shown in the third row in Fig. 8, almost all samples in the Count and Position task are located above the $y = x$ line.

In our paradigm, MLLMs are allowed to retrospect visual references that are semantically accordant to the image. We expect the comparison with such *standard answers* can help reduce false positives. Figure 8 illustrates that after integrating *Pensieve* (in the second and fourth row), there are fewer red triangle

marks above the $y = x$ line, *i.e.*, less false positives, especially in the Color subtask. This indicates that the number of false positives is reduced.

C.4 More Results on POPE

Detailed results on three official splits of POPE benchmark (the random, popular, and adversarial splits) are shown in Tab. 7. *Pensieve* boosts the accuracy and the F1 score for both LLaVA1.5 and InstructBLIP on almost all splits of all subsets (COCO, AOKVQA and GQA), exceeding DoLa and VCD in varying degrees. We notice *Pensieve*'s impact on InstructBLIP slightly oscillates in the COCO subset, while the performance is consistently better than VCD.

Table 7: Results on the POPE benchmark MSCOCO, AOKVQA and GQA subsets. We report the performance in random, popular, and adversarial settings. *Pensieve* improves the overall performance for both MLLMs.

Setting	Model	Decoding	COCO		AOKVQA		GQA	
			Acc. \uparrow	F1 \uparrow	Acc. \uparrow	F1 \uparrow	Acc. \uparrow	F1 \uparrow
Random	LLaVA-1.5	greedy	87.13	85.58	88.73	88.16	89.33	88.81
		+DoLa	86.93	85.31	88.66	88.06	89.30	88.74
		+VCD	88.63	88.15	87.16	87.46	88.03	88.43
	InstructBLIP	+Ours	87.53	86.17	89.20	88.84	89.46	89.16
		greedy	87.97	86.97	88.50	88.54	87.26	87.31
		+DoLa	88.00	87.03	88.50	88.57	87.23	87.29
Popular	LLaVA-1.5	+VCD	87.07	85.97	86.80	86.97	86.37	86.38
		+Ours	87.83	86.79	88.53	88.54	87.23	86.70
		greedy	85.90	84.41	85.30	85.09	84.00	84.12
	InstructBLIP	+DoLa	85.70	84.14	85.30	85.05	84.00	84.05
		+VCD	86.13	85.93	83.07	83.94	82.43	83.85
		+Ours	86.13	84.87	85.57	85.62	84.53	84.89
Adversarial	LLaVA-1.5	greedy	84.97	84.24	81.86	83.05	78.60	80.37
		+DoLa	85.06	84.36	81.86	83.09	78.57	80.37
		+VCD	84.43	83.62	81.63	82.77	79.87	81.15
	InstructBLIP	+Ours	84.90	84.12	82.03	83.16	80.20	80.78
		greedy	83.63	82.33	78.93	79.94	80.87	81.58
		+DoLa	83.50	82.12	78.93	79.87	80.83	81.48
Adversarial	LLaVA-1.5	+VCD	82.00	82.51	75.96	78.75	78.03	80.62
		+Ours	83.73	82.70	78.90	80.29	81.00	82.09
		greedy	82.50	82.15	74.83	77.93	75.87	78.40
	InstructBLIP	+DoLa	82.56	82.24	74.86	78.00	75.86	78.42
		+VCD	81.77	81.27	76.06	78.61	76.47	78.63
		+Ours	82.63	82.21	74.93	77.96	77.83	78.98

C.5 More Ablations

Token Sampling. In the main paper, greedy search is used as the baseline decoding strategy, *i.e.*, always selecting the candidate with the highest confidence score. We further study the integration of *Pensieve* with different token sampling strategies in Tab. 8. Greedy search avoids errors induced by token sampling and

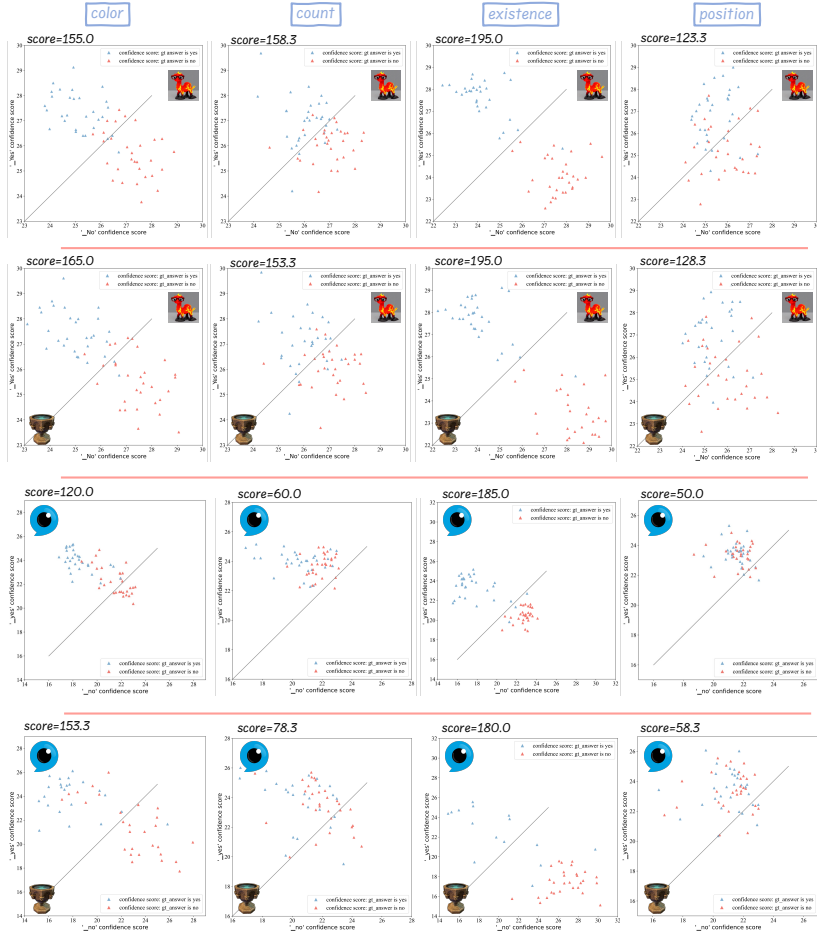


Fig. 8: Case study for the impact of *Pensieve* on the MME benchmark. We plot the confidence scores corresponding to the candidates `_yes` and `_no` on the vertical and horizontal axis, respectively. Each test sample corresponds to a blue or red triangle mark, indicating that the ground truth answer is `_yes` or `_no`, respectively. Our proposed *Pensieve* reduces false positives on four hallucination subtasks of the MME benchmark. Best viewed in color and zoomed in.

thus has the highest performance. Our proposed *Pensieve* can be well integrated with various sampling strategies, enhancing image captioning performance and reducing visual hallucination. For nucleus (Top-p) sampling, we set $p = 0.9$. For Top-k sampling, we set $k = 50$. We fix the random seeds in all experiments.

Table 8: Token sampling experiments on Whoops benchmark. *Pensieve* enhances the performance for LLaVA-1.5 across various baseline decoding strategies, including greedy search and different token sampling methods.

Method	B4 ↑	M ↑	C ↑	S ↑	FS% ↑	
<i>zeroshot</i>						
LLaVA-1.5 Vicuna-7B	greedy	19.7	25.6	67.9	17.3	67.9
	+ <i>Ours</i>	20.0	26.3	75.5	17.8	68.3
	sample	6.9	19.0	31.4	12.0	57.8
	+ <i>Ours</i>	8.8	20.3	40.6	13.7	61.9
	nucleus	9.6	20.5	39.4	13.3	62.4
	+ <i>Ours</i>	10.7	21.8	46.8	14.0	65.4
	Top-k	8.0	19.3	33.6	12.3	59.1
	+ <i>Ours</i>	8.8	20.3	40.6	13.7	62.4

D More Examples to Support our Premise

In this section, we provide more examples to support our claim that MLLMs may not be utterly ignorant of accurate visual cues when they hallucinate. Moreover, images with similar semantics and appearance can induce analogous visual hallucinations in the same context, and token candidates with sharper variation in confidence score distribution are more likely to be the accurate ones.

We first provide two examples with the test image from the OpenImages [24] validation set in Fig. 9 and Fig. 10. For the hallucinated content *_zoo* and *_ban*, which ranks first in the vocabulary, the visual branch contributed +5.117 and +5.922 *img scores*, respectively. Meanwhile, the visual modality also contributes comparable *img scores* for the accurate candidates, *e.g.*, +4.703 scores for *_f* (the first token for fence, ranks second), and +3.898 for *_m* (the first token for mango, ranks third). This indicates that the MLLM is aware of the accurate visual cues amidst hallucination, whereas the visual branch also mistakenly advocated other erroneous candidates. In these scenarios, directly implementing VCD may further exacerbate visual hallucinations, as the *img scores* of the hallucinatory candidates are higher than that of the accurate ones.

In Fig. 9 and Fig. 10, we also observe analogous visual hallucinations among similar images, *e.g.*, *_zoo*, *_c* (first token for cage), and *_pen* in Figure 9, as well as *_ban* and *_un* (first token for unripe) in Figure Fig. 10. These hallucinatory candidates obtain relatively high confidence scores even though the input images **do not** contain such visual information. Moreover, another notable phenomenon emerges: the accurate candidates’ *kNN scores* are significantly lower than that of the erroneous candidates, *e.g.*, the accurate candidate *_f*’s confidence score

dropped from 16.328 to 9.529 in average. This change is more significant than the hallucinatory candidates, *e.g.*, `_zoo` from 17.719 to 17.137, `_c` from 16.313 to 12.813, and `_pen` from 15.328 to 12.732. This difference can help distinguish the accurate content from hallucinations.

We provide more examples in Figures Fig. 11 to Fig. 15, with test images from the Whoops benchmark, LLaVA Bench in the wild, and crawled from the internet. These examples further validates our three main claims:

- **MLLMs are not completely ignorant of the accurate visual cues amidst visual hallucination.** In Fig. 11 to Fig. 15, we notice that at least one accurate candidate consistently ranks among the top-3 most probable candidates in \mathcal{V}_{head}^m , with comparable confidence score to the top-ranked candidates, *e.g.*, `_hot` gets 15.406 scores and ranks second (-0.032 compared to top one) in Fig. 11, `_rub` scores 19.203 and ranks second (-0.375 compared to top one) in Fig. 12, `_fuel` scores 13.695 and ranks second (-0.304 compared to top one) in Fig. 13, `_smoke` scores 17.547 and ranks second (-0.328 compared to top one) in Fig. 14, `_y` (first token for yogurt) and `_st` (first token for strawberry) score 16.625 (-0.531 compared to top one) and 16.406 (-0.422 compared to top one), respectively, in Fig. 15. In other words, the hallucinatory candidates marginally exceed the faithful ones and lead to visual hallucinations in the responses. This observation validates the feasibility of mitigating visual hallucinations by moderately adjusting the predicted confidence score distribution.
- **Similar Images can Induce Analogous Visual Hallucination.** In Fig. 11 to Fig. 15, we observe that in the same context, analogous visual hallucination can occur among images with similar semantic and appearance characteristics. Specifically, hallucinatory candidates may get one or more high *kNN score* even though they can **not** be grounded in the corresponding *kNN* image. For instance, in Fig. 11, candidate `_c` and `_l` (first token for lollipop) have more than 14 confidence scores in the third and fourth visual references that contain only children and toothbrushes. In Fig. 12, candidate `_du` scores 20.063 and 19.838 in the first and third references, respectively, which contain swans only. In Fig. 13, candidate `_fire` scores more than 10 in images without fire-related content, and `_person` scores 12.984 and 12.180 in images without people, which is very close to the predicted scores when the input images do contain people (13.344 and 13.188). In Fig. 14, the ambiguous candidate `_two` scores from 12.273 to 15.531 across images crowded with multiple objects. In Fig. 15, candidates `_ju` (first token for juice), `_orange`, and `_bow` have high confidence scores across all reference images, yet some of the references do not contain such visual content. Note that we do not deny that candidates with high *kNN scores* across all references can be the correct content that the references have in common, we pinpoint our observation that they are more likely to be hallucinations compared to candidates with significant score changes.
- **Visual References Help Discern Accurate Content.** Compared to the candidates with subtle confidence score changes, we claim that candidates

with more significant score variation are *more likely* to be the accurate ones. For instance, in Fig. 11, the accurate candidate *_hot*'s score changed from 15.406 to 11.428 in average, where as the hallucinatory candidate *_c*'s score changed from 15.438 to 14.820. in Fig. 12, the accurate candidate *_rub*'s score changed from 19.203 to 8.857 in average, which is much more drastic than that of other hallucinatory (e.g., *_du* from 19.578 to 17.609) or ambiguous (*_baby* from 18.984 to 15.943) candidates. In Fig. 13, Fig. 14, and 15, we also observe that the *kNN scores* of all accurate candidates (marked with a star emoji) are significantly *lower* than that of other erroneous candidates with close ranks in the vocabulary, e.g., *_fuel*, *_gas*, and *_tank* in Fig. 13, *_smoke*, *_fl* (first token for flame), and *_fire* in Fig. 14, as well as *_y*, *_st*, and *_left* in Fig. 15. This phenomenon could be leveraged to discern the accurate content from hallucinations. In practice, we contrast the scores predicted by the test images to other scores predicted by the retrieved similar images, thereby promoting the candidates that are more likely to be the faithful ones. Note that we do *not* pre-establish or assume certain candidates to be the correct ones. Instead, we involve all top-50 ranked candidates in \mathcal{V}_{head}^m for score comparison, facilitating MLLMs to discern *multiple potentially correct* candidates by comparing similar but non-identical images.

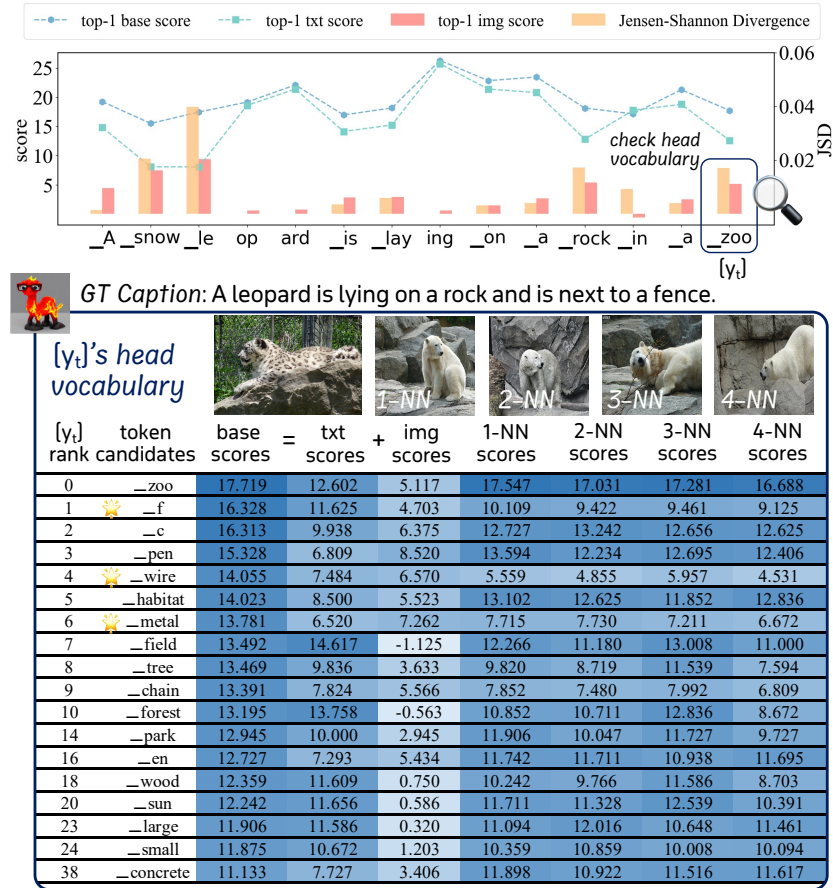


Fig. 9: More qualitative evidence to support our hypothesis. This caption is predicted by LLaVA1.5-7B. The test image is from the OpenImages validation set, and the references are from the COCO Caption dataset. The star emojis indicate the accurate candidates.

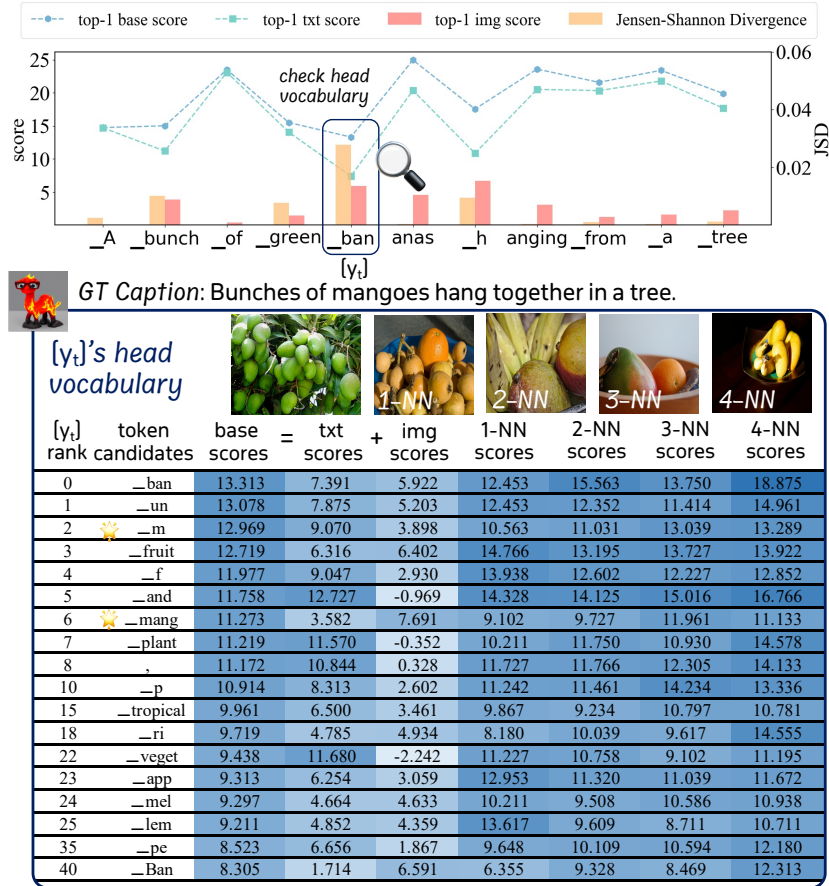


Fig. 10: More qualitative evidence to support our hypothesis. This caption is predicted by LLaVA1.5-7B. The test image is from the OpenImages validation set, and the references are from the COCO Caption dataset. The star emojis indicate the accurate candidates.

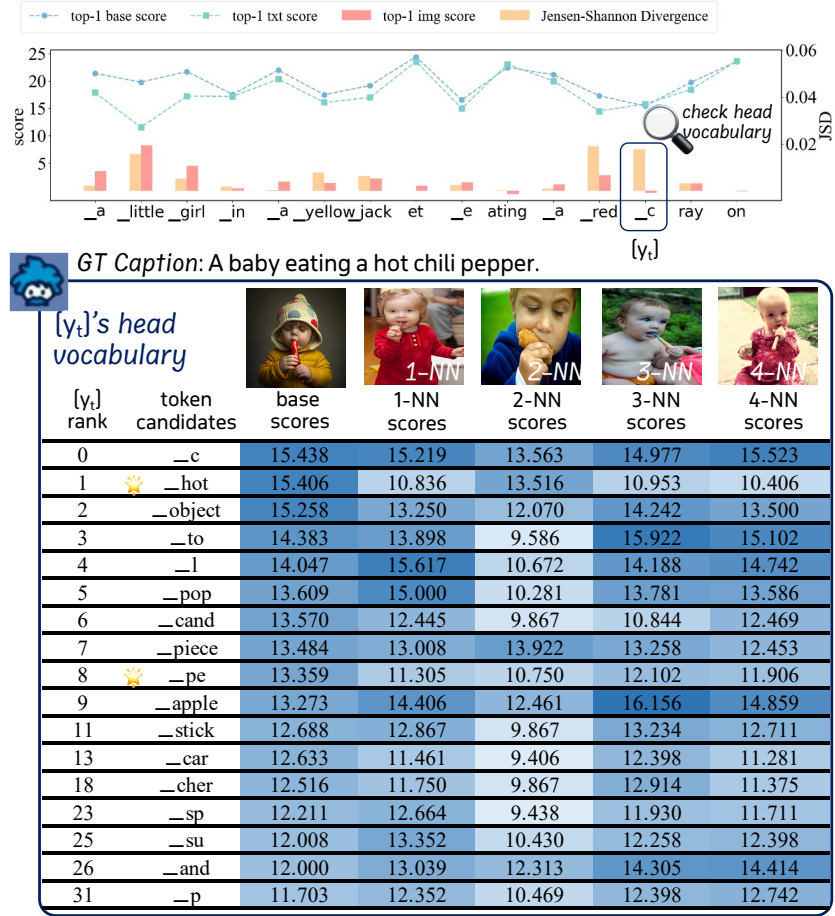


Fig. 11: More qualitative evidence to support our hypothesis. This caption is predicted by InstructBLIP-Vicuna-7B. The test image is from the Whoops benchmark, and the references are from the COCO Caption dataset. The star emojis indicate the accurate candidates.

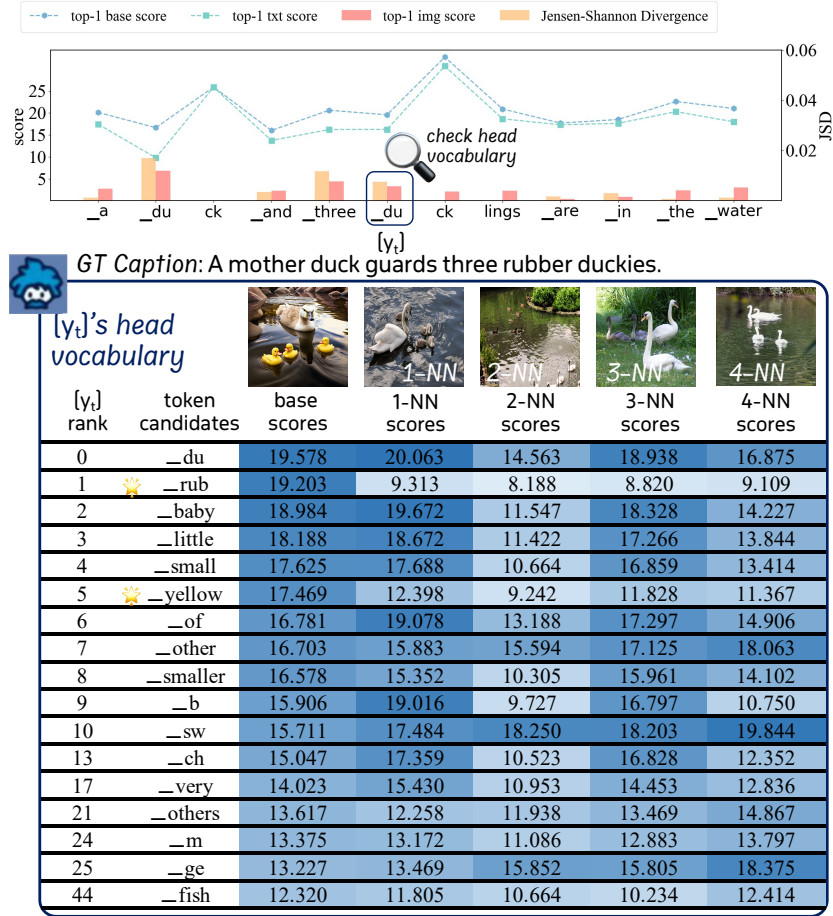


Fig. 12: More qualitative evidence to support our hypothesis. This caption is predicted by InstructBLIP-Vicuna-7B. The test image is from the Whoops benchmark, and the references are from the COCO Caption dataset. The star emojis indicate the accurate candidates.

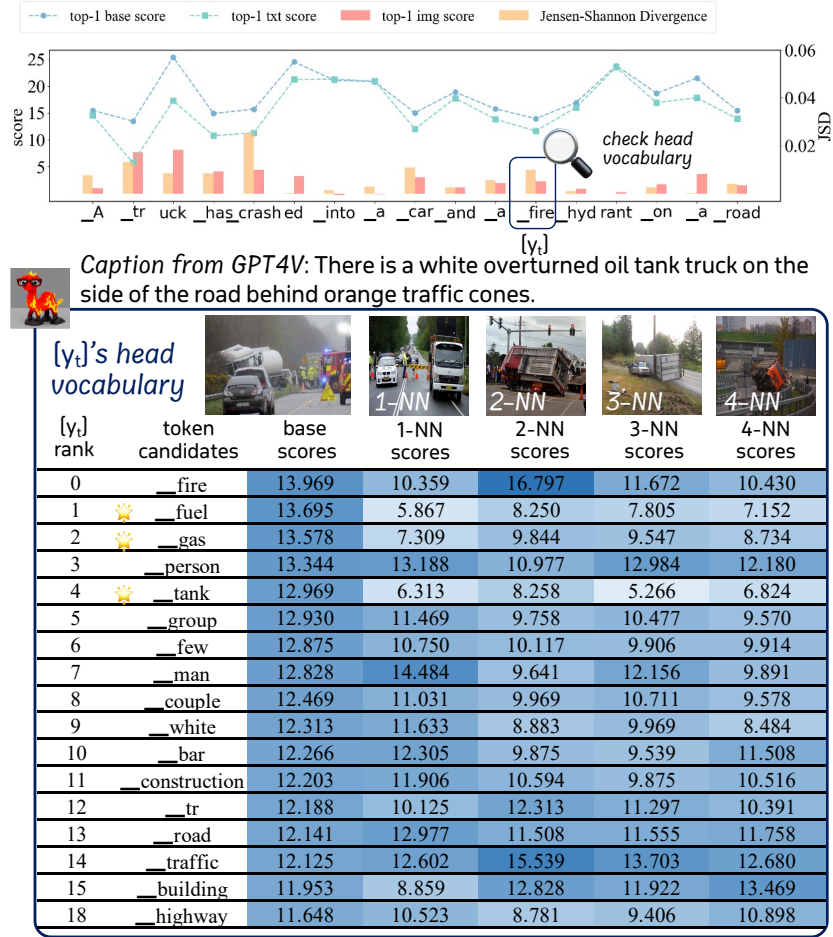
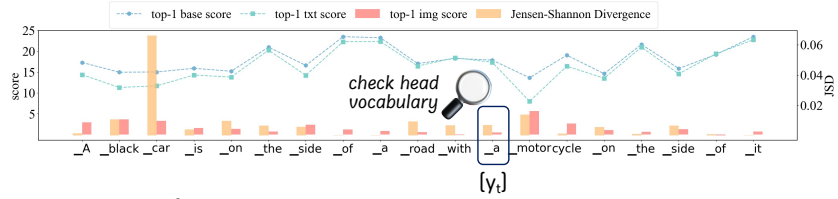
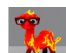


Fig. 13: More qualitative evidence to support our hypothesis. This caption is predicted by LLaVA1.5-7B. The test image is crawled from the internet, and the references are from the COCO Caption dataset. The star emojis indicate the accurate candidates.



 *Caption from GPT4V*: A black car is shown after an accident, with visible damage and smoke rising from the front.

[y_t]'s head vocabulary

[y _t] rank	token candidates	base scores	1-NN scores	2-NN scores	3-NN scores	4-NN scores
0	__a	17.875	16.906	17.844	15.789	18.156
1	🌟 __smoke	17.547	8.844	7.785	12.422	9.547
2	__its	17.047	10.648	11.703	12.711	12.195
3	🌟 __fl	16.094	7.328	9.102	7.535	8.313
4	__the	16.031	13.391	14.578	13.820	15.430
5	__an	15.672	14.133	16.016	13.516	15.375
6	🌟 __fire	15.094	6.852	7.398	6.965	7.234
7	__yellow	14.938	12.000	11.781	11.344	12.805
8	__some	14.539	12.664	13.430	12.313	13.516
9	__it	14.531	9.445	10.250	10.266	11.133
10	__no	14.422	12.250	11.844	11.789	12.969
11	__grass	14.219	8.609	10.695	7.980	9.211
12	__two	13.961	13.734	15.531	12.273	15.250
14	__sm	13.828	8.273	7.824	11.602	8.508
15	__people	13.805	10.086	10.297	11.523	11.672
19	__signs	13.453	14.453	14.961	11.344	15.078
21	__black	13.320	10.180	11.313	9.766	11.422

Fig. 14: More qualitative evidence to support our hypothesis. This caption is predicted by LLaVA1.5-7B. The test image is crawled from the internet, and the references are from the COCO Caption dataset. The star emojis indicate the accurate candidates.



GT Caption: An open refrigerator filled with a variety of food items. In the left part of the compartment, towards the front, there is a plastic box of strawberries with a small bag of baby carrots on top. Towards the back, there is a stack of sauce containers. In the middle part of the compartment, towards the front, there is a green plastic box, and there is an unidentified plastic bag placed on it. Towards the back, there is a carton of milk. In the right part of the compartment, towards the front, there is a box of blueberries with three yogurts stacked on top. The large bottle of yogurt is Fage non-fat yogurt, and one of the smaller cups is Fage blueberry yogurt. The brand and flavor of the other smaller cup are unknown. Towards the back, there is a container with an unknown content.

Pred: ["_The", "_image", "_displays", "_a", "_re", "fr", "iger", "ator", "_filled", "_with", "_various", "_food", "_items", "_and", "_drink", "s", "_inside", "_the", "_re", "fr", "iger", "ator", "_there", "_are", "_multiple", "_bott", "les", "_including", "_milk", "_and"]
[y_p]

Pred: ["_The", "_image", "_displays", "_a", "_re", "fr", "iger", "ator", "_filled", "_with", "_various", "_food", "_items", "_and", "_drink", "s", "_inside", "_the", "_re", "fr", "iger", "ator", "_there", "_are", "_multiple", "_bott", "les", "_including", "_milk", "_and", "_ju", "ice", "_placed", "_in", "_different", "_compart", "ments", "_Some", "_of", "_the", "_bott", "les", "_are", "_located", "_on", "_the", "_top", "_sh", "elf", "_while", "_others", "_are", "_placed", "_on", "_the", "_middle", "_and", "_bottom", "_sh", "elf", "ves", "s", "k0x0A", "k0x0A", "in", "_addition", "_to", "_the", "_bott", "les", "_there", "_are", "_several", "_car", "ro", "ts", "_and", "_a"]
[y_a]

[y _p] rank	token candidates	base scores	1-NN scores	2-NN scores	3-NN scores	4-NN scores
0	_ju	17.156	17.875	17.516	16.563	16.750
1	_y	16.625	12.359	12.484	12.750	12.227
2	_other	14.938	15.594	15.547	14.648	15.547
3	_orange	14.766	15.008	15.617	14.086	14.570
4	_a	14.492	14.625	14.602	14.430	15.031
5	_water	14.492	15.953	17.203	15.531	15.094
6	_possibly	14.063	14.094	14.133	13.422	14.328
7	_some	13.672	14.414	14.188	13.500	14.250
8	_ere	13.359	12.102	10.164	10.055	12.484
9	_fruit	13.172	13.695	13.680	11.352	11.406
11	_ice	12.805	10.969	10.188	10.633	10.930
14	_several	12.609	13.500	13.664	12.953	13.609
16	_two	12.453	11.945	12.234	12.133	12.438
17	_milk	12.297	11.750	8.656	13.469	11.461
19	_wine	12.227	14.250	14.273	12.883	14.172
21	_eggs	12.125	11.945	11.281	14.469	10.969
42	_apple	10.969	12.391	12.313	10.922	11.086

[y _a] rank	token candidates	base scores	1-NN scores	2-NN scores	3-NN scores	4-NN scores
0	_bow	16.828	18.328	16.563	15.867	16.688
1	_st	16.406	10.227	14.531	10.172	8.969
2	_cup	15.555	15.773	14.867	14.969	15.375
3	_few	15.156	15.039	14.977	14.273	13.906
4	_ban	14.859	15.516	15.648	14.430	14.133
5	_container	14.625	12.578	11.961	12.414	12.078
6	_couple	14.469	14.805	14.945	14.289	13.977
7	_cart	14.461	13.516	12.117	13.203	11.875
8	_bunch	14.438	14.313	14.133	13.680	12.859
9	_bag	14.227	13.016	13.680	14.047	13.547
10	_package	13.977	12.203	11.891	12.359	12.289
11	_box	13.977	11.430	10.914	11.055	12.125
12	_sp	13.906	13.953	13.555	12.852	13.438
16	_large	13.258	13.258	13.406	12.656	12.672
17	_small	13.234	13.438	12.922	12.625	12.336
31	_slice	12.000	12.820	13.953	13.016	12.594
37	_jar	11.727	11.344	11.094	11.266	11.492

Pred: ["_The", "_image", "_displays", "_a", "_re", "fr", "iger", "ator", "_filled", "_with", "_various", "_food", "_items", "_and", "_drink", "s", "_inside", "_the", "_re", "fr", "iger", "ator", "_there", "_are", "_multiple", "_bott", "les", "_including", "_milk", "_and", "_ju", "ice", "_placed", "_in", "_different", "_compart", "ments", "_Some", "_of", "_the", "_bott", "les", "_are", "_located", "_on", "_the", "_top", "_sh", "elf", "_while", "_others", "_are", "_placed", "_on", "_the", "_middle", "_and", "_bottom", "_sh", "elf", "ves", "s", "k0x0A", "k0x0A", "in", "_addition", "_to", "_the", "_bott", "les", "_there", "_are", "_several", "_car", "ro", "ts", "_and", "_a", "_bow", "t", "_of", "_st", "raw", "ber", "ries", "_placed", "_in", "_the", "_re", "fr", "iger", "ator", "_The", "_car", "ro", "ts", "_are"]
[y_p]

Pred: ["_The", "_image", "_displays", "_a", "_re", "fr", "iger", "ator", "_filled", "_with", "_various", "_food", "_items", "_and", "_drink", "s", "_inside", "_the", "_re", "fr", "iger", "ator", "_there", "_are", "_multiple", "_bott", "les", "_including", "_milk", "_and", "_ju", "ice", "_placed", "_in", "_different", "_compart", "ments", "_Some", "_of", "_the", "_bott", "les", "_are", "_located", "_on", "_the", "_top", "_sh", "elf", "_while", "_others", "_are", "_placed", "_on", "_the", "_middle", "_and", "_bottom", "_sh", "elf", "ves", "s", "k0x0A", "k0x0A", "in", "_addition", "_to", "_the", "_bott", "les", "_there", "_are", "_several", "_car", "ro", "ts", "_and", "_a", "_bow", "t", "_of", "_st", "raw", "ber", "ries", "_placed", "_in", "_the", "_re", "fr", "iger", "ator", "_The", "_car", "ro", "ts", "_are", "_scattered", "_throughout", "_the", "_re", "fr", "iger", "ator", "_with", "_some", "_on", "_the", "_top", "_sh", "elf", "_and", "_others", "_on", "_the", "_middle", "_and", "_bottom", "_sh", "elf", "ves", "s", "_The", "_bow", "t", "_of", "_st", "raw", "ber", "ries", "_is", "_placed", "_on", "_the"]
[y_a]

[y _p] rank	token candidates	base scores	1-NN scores	2-NN scores	3-NN scores	4-NN scores
0	_scattered	16.781	17.422	17.359	17.172	17.375
1	_spread	16.391	16.406	16.656	16.625	16.641
2	_located	16.156	16.750	16.484	16.563	16.500
3	_distributed	15.883	16.094	16.219	16.188	16.141
4	_arranged	15.563	15.195	15.242	15.305	15.273
5	_found	15.367	15.664	15.523	15.508	15.516
6	_position	15.180	15.523	15.266	15.320	15.375
7	_placed	15.156	15.219	15.039	15.133	15.125
8	_situated	14.961	15.359	15.047	15.148	15.086
9	_in	14.406	14.039	14.055	14.117	14.148
10	_stored	14.242	13.031	12.867	13.281	13.047
12	_dispers	14.055	14.695	14.789	14.578	14.727
13	_on	13.938	14.281	13.945	14.125	13.969
15	_even	13.594	13.750	13.758	13.695	13.719
16	_organized	13.523	12.758	12.719	12.945	12.711
21	_pack	12.539	11.320	11.328	11.508	11.359
27	_mixed	11.930	12.078	12.148	12.133	12.156

[y _a] rank	token candidates	base scores	1-NN scores	2-NN scores	3-NN scores	4-NN scores
0	_bottom	22.609	22.547	22.047	22.547	21.922
1	_middle	21.453	21.953	22.844	22.453	22.266
2	_lower	20.953	20.625	20.484	20.672	20.469
3	_top	20.703	20.984	21.453	21.172	21.625
4	_left	19.813	18.203	18.125	17.875	18.719
5	_right	18.531	19.156	17.484	18.172	19.234
6	_upper	18.516	18.859	19.359	18.922	19.609
7	_sh	18.375	18.141	18.375	18.047	17.969
8	_door	18.266	17.688	17.484	17.828	17.797
9	_same	17.500	17.203	17.469	17.359	17.438
11	_second	17.125	16.969	17.688	17.156	16.969
12	_lowest	16.859	16.719	16.359	16.828	16.297
13	_front	16.578	16.188	15.609	16.016	16.203
14	_counter	16.531	16.047	16.047	16.203	16.531
15	_far	16.344	16.234	14.680	15.172	16.172
18	_floor	15.828	15.930	15.516	15.625	15.547
19	_third	15.758	15.859	16.344	15.930	15.688

Prediction: The image displays a refrigerator filled with various food items and drinks. Inside the refrigerator, there are multiple bottles, including milk and juice, placed in different compartments. Some of the bottles are located on the top shelf, while others are placed on the middle and bottom shelves. In addition to the bottles, there are several carrots and a bowl of strawberries placed in the refrigerator. The carrots are scattered throughout the refrigerator, with some on the top shelf and others on the middle and bottom shelves. The bowl of strawberries is placed on the bottom shelf, adding a touch of color to the refrigerator's contents.

Fig. 15: More qualitative evidence to support our hypothesis. This sample is from the LLaVA Bench in the wild [39] benchmark. Hallucinatory content is marked red.